Insights on the antiviral mechanisms of action of the TLR1/2 agonist Pam3CSK4 in hepatitis B virus (HBV)-infected hepatocytes

Manon Desmares, Marion Delphin, Brieux Chardès, Caroline Pons, Juliette Riedinger, Maud Michelet, Michel Rivoire, Bernard Verrier, Anna Salvetti, Julie Lucifora, et al.

▶ **To cite this version:**

Manon Desmares, Marion Delphin, Brieux Chardès, Caroline Pons, Juliette Riedinger, et al.. Insights on the antiviral mechanisms of action of the TLR1/2 agonist Pam3CSK4 in hepatitis B virus (HBV)-infected hepatocytes. Antiviral Research, 2022, 206, pp.105386. 10.1016/j.antiviral.2022.105386 . hal-03869860

HAL Id: hal-03869860
https://hal.science/hal-03869860

Submitted on 24 Nov 2022

HAL is a multi-disciplinary open access archive for the deposit and dissemination of scientific research documents, whether they are published or not. The documents may come from teaching and research institutions in France or abroad, or from public or private research centers.

L'archive ouverte pluridisciplinaire **HAL**, est destinée au dépôt et à la diffusion de documents scientifiques de niveau recherche, publiés ou non, émanant des établissements d'enseignement et de recherche français ou étrangers, des laboratoires publics ou privés.

Insights on the antiviral mechanisms of action of the TLR1/2 agonist Pam3CSK4 in hepatitis B virus (HBV)-infected hepatocytes

Manon Desmares[1], Marion Delphin[1,$], Brieux Chardès[1,$], Caroline Pons[1,2], Juliette Riedinger[2], Maud Michelet[1], Michel Rivoire[3], Bernard Verrier[4], Anna Salvetti[1,2], Julie Lucifora[1,2,#] and David Durantel[1,2,#]

[1] INSERM, U1052, Cancer Research Center of Lyon (CRCL), University of Lyon (UCBL1), CNRS UMR_5286, Centre Léon Bérard, Lyon, France;
[2] INSERM, U1111, Centre International de Recherche en Infectiologie (CIRI), University of Lyon (UCBL1), CNRS UMR_5308, ENS de Lyon, Lyon, France ;
[3] INSERM U1032, Centre Léon Bérard (CLB), Lyon, France;
[4] Laboratoire de Biologie tissulaire et Ingénierie Thérapeutique, CNRS UMR_5305, University of Lyon (UCBL1), Lyon, France.

[$] Contributed equally
[#] Contributed equally

Correspondence
Dr. Dr. David Durantel
INSERM, U1111, Centre International de Recherche en Infectiologie (CIRI), University of Lyon (UCBL1), CNRS UMR_5308, ENS de Lyon, 21 Avenue Tony Garnier, Lyon, F-69007, France. Phone: + 33 6 82 50 91 87; E-mail: david.durantel@inserm.fr

Key Words
Hepatitis B virus; hepatocytes; toll-like receptor 1/2; TLR2 agonist; antiviral activity; NF-κB pathway; FEN-1.

Electronic word count (without references and figures legends): 6360
Number of figures: 6
Number of supplementary figures: 14

Author contributions
- Study concept and design: DD, JL
- Acquisition and analyses of data: MDes, MDel, BC, CP, JR, MM
- Interpretation of data: MDes, MDel, BC, JL, DD
- Drafting and revision of the manuscript: DD, MDes, JL, AS
- Funding acquisition: DD, JL, BV
- Material support: MR, BV

Financial support
This work was supported by two grants from the CSS12 of ANRS (Agence Nationale pour la Recherche sur le Sida et les Hépatites Virales, ECTZ65108 and ECTZ137751), an Infect-Era European grant, operated by ANR (Agence Nationale pour la Recherche; ANR 16-IFEC-0005-01), as well as core financial support from INSERM, CNRS, and University of Lyon. This work was also supported by the DEVweCAN LABEX (ANR-10-LABX-0061) of the "Université de Lyon", within the program "Investissements d'Avenir" (ANR-11-IDEX-0007) operated by ANR.

Competing financial interest
none

Abstract

Objectives: Pegylated-interferon-alpha (Peg-IFNα), an injectable innate immune protein, is still used to treat chronically HBV-infected patients, despite its poor tolerability. Peg-IFNα has the advantage over nucleos(t)ide analogues (NAs) to be administrated in finite regimen and to lead to a higher HBsAg loss rate. Yet it would be interesting to improve the efficacy (i.e. while decreasing doses), or replace, this old medicine by novel small molecules/stimulators able to engage innate immune receptors in both HBV replicating hepatocytes and relevant innate immune cells. We have previously identified the Toll-Like-Receptor (TLR)-2 agonist Pam3CSK4 as such a potential novel immune stimulator. The aim of this study was to gain insights on the antiviral mechanisms of action of this agonist in *in vitro* cultivated human hepatocytes.

Design: We used *in vitro* models of HBV-infected cells, based on both primary human hepatocytes (PHH) and the non-transformed HepaRG cell line to investigate the MoA of Pam3SCK4 and identify relevant combinations with other approved or investigational drugs.

Results: We exhaustively described the inhibitory anti-HBV phenotypes induced by Pam3CSK4, which include a strong decrease in HBV RNA production (inhibition of synthesis and acceleration of decay) and cccDNA levels. We confirmed the long-lasting anti-HBV activity of this agonist, better described the kinetics of antiviral events, and demonstrated the specificity of action through the TLR1/2- NF-κB canonical-pathway. Moreover, we found that FEN-1 could be involved in the regulation and inhibitory phenotype on cccDNA levels. Finally, we identified the combination of Pam3CSK4 with IFNα or an investigational kinase inhibitor (called 1C8) as valuable strategies to reduce cccDNA levels and obtain a long-lasting anti-HBV effect *in vitro*.

Conclusions: TLR2 agonists represent possible assets to improve the rate of HBV cure in patients. Further evaluations, including regulatory toxicity studies, are warranted to move toward clinical trials.

Introduction

According to WHO, more than 250 million individuals are concerned worldwide by chronic hepatitis B infection. If left untreated, these individuals are at risk of developing life-threatening liver diseases, including cirrhosis and hepatocellular carcinoma (HCC) [1, 2]. An estimated 5% of chronic carriers are diagnosed patients and can benefit from a treatment [1]. In the richest countries that benefit from advanced medical systems, nucleosides analogues (NAs; *e.g.* Entecavir, Tenofovir…), which are very safe and easy to use (*per os* administration) antivirals specifically targeting the HBV polymerase, represent the main treatment option [3, 4]. Even if very efficient at reducing viremia and the risk of development of HBV-associated liver diseases, these drugs need to be taken long-term to prevent virological relapses and do not lead to a high rate of HBsAg loss, which is currently viewed as the best marker of a *functional cure* in chronic hepatitis B patients (CHB) [4]. Pegylated-interferon-alpha (Peg-IFNα), an injectable innate immune cytokine/stimulator, was historically the first drug used to treat CHB and is still used, in monotherapy or combination with NAs, in some countries [5]. Despite numerous side effects and an overall poor tolerability in patients, Peg-IFNα has the advantage over NAs to be administrated in finite regimen (usually 48 weeks) and to lead to a higher HBsAg loss rate (between 5 and 10%) [4, 5]. Moreover, Peg-IFNα is a backbone regimen to treat CHB patients who are co/super-infected with the hepatitis Delta virus (HDV) [6]. Recent clinically trialed combinations of Peg-IFNα with either an HBV/HDV entry inhibitor (Bulevirtide) or nucleic acid polymers (NAPs; e.g. REP2139) clearly indicate that this innate immune cytokine/stimulator is likely to remain in the therapeutic landscape for HBV/HDV chronic infections [7-9]. Yet, it would be interesting to keep the advantage of an innate immune stimulator while getting rid of the side effects of Peg-IFNα. This is the reason why a strong attention has been paid to pattern recognition receptor (PRR) agonists as potential novel components of combination therapies for HBV/HDV chronic infections [3, 10, 11].

Following an older study made in HBV transgenic mice [12], we have recently screened the *in vitro* antiviral properties a various toll-like receptor (TLR) agonists in HBV-infected hepatocytes, cultivated

in the absence of any innate immune cells in order to identify those capable to directly act on HBV replication [13]. We identified Pam3CSK4, a well-known TLR1/2 agonist as one of the best molecule to inhibit HBV replication in both differentiated HepaRG cells [14] and freshly isolated primary human hepatocytes (PHH) [15], which are both non-transformed/non-cancerous hepatocytes, yet fully functional for innate immune pathways [16-18]. In this study, using the same relevant cell culture models, we aimed at getting insights on the mechanisms of action of the TLR1/2 agonist, Pam3CSK4. We confirmed the long-lasting anti-HBV activity of this agonist, better described the kinetics of antiviral events, demonstrated the specificity of action through the TLR1/2- NF-κB canonical-pathway, and identified a host factor involved, at least partially, in the inhibitory phenotype on cccDNA levels. Finally, we evaluated the potential combination of Pam3CSK4 with approved (NAs, IFNα), currently trialed (CAMs, FXR agonist) and investigational (kinase inhibitor) drugs, as this strategy is expected to be the way forward to foster HBV cure in patients [3, 4].

Methods

Main reagents and chemicals

Pam3CSK4 (TLR-1/2 agonist) was purchased from InvivoGen, IFN-α (Roferon) from Roche, Tenofovir and RG7834 from Ai-Biopharma (Montpellier, France), GW4064 (FXR agonist) from Selleckem, and 1C8 from AVG Discovery (Montpellier, France). Core assembly modulators (CAMs) JNJ-827 and JNJ-890 were described in [19] and obtained from Janssen. Others chemical reagents (cycloheximide, triptolide etc…) were obtained from Sigma-Aldrich. To activate LTβ-R and the NF-κB non-canonical pathway, we used a super-agonistic tetravalent bi-specific antibody (BS1) described in [20], and kindly provided by Pr Mathias Heikenwalder (Univ. Heidelberg, Germany). Antibodies were purchased from Cell Signaling (against TLR1, TLR2, TLR3, TLR6, NF-κB p65, pp65, p52, RelB, p50), Abcam (against FEN-1 and HNF4α), Gene Tex (against MCPIP1), Sigma-Aldrich (against beta actin), and Dako (against HBc and secondary antibodies). The full list with references is given in the ***supplementary material and methods*** section. Smartpool siRNAs were purchased from Darmacon; the list of siRNAs used is provided in the ***supplementary material and methods*** section. Primers for qPCR and RT-qPCR were mainly purchased from Eurogentec. The list with sequences information is provided in the ***supplementary material and methods*** section.

Cell culture and HBV infection

HepaRG cells were cultured, differentiated, and infected by HBV as previously described [14, 21]. PHH were freshly prepared from human liver resections obtained from the Centre Léon Bérard (Lyon) with French ministerial authorizations (AC 2013-1871, DC 2013 – 1870, AFNOR NF 96 900 sept 2011) as previously described [15].

Genotype D HBV inocula were prepared from HepAD38 supernatants [22]. HBV genotype C inocula was prepared from home-made HepG2 cell lines. A plasmid (pcDNA 3.1 + from Thermo Fisher Scientific, which contain a neomycin resistant gene) containing 1.35 genome unit of consensus

genotype C sequence (extracted from the HBV database: https://hbvdb.lyon.inserm.fr/HBVdb/) was linearized and transfected into HepG2-ATCC cells. A polyclonal cell line resistant to G418 (500 µg/mL) was initially obtained and frozen. Then, two rounds of cell cloning were performed by an end-point dilution method (i.e. plating of cells in collagen treated large petri dish at very low density leading to the formation of cell colonies, which could be scratched and grown individually). One cell line was thus generated and used for the production of genotype C HBV inocula. Supernatants containing HBV particles were concentrated with 8% PEG 8000 (Sigma-Aldrich). In contrast to inocula prepared with HepAD38 supernatants, inocula prepared from this cell line led to titer at $1x10^9$ virus genome equivalent (vge) after PEG concentration. Infection of HepaRG cells were done using between 10 and 100 vge/cell. All virus preparations were tested for the absence of endotoxin (Lonza). Concentrated viruses were characterized by analysis of the fractions from 20-44% iodixanol gradients. Of note, the rate of cells infection (dHepaRG and PHH) varies from one batch/donor to another. Data are therefore mostly presented as ratio to non-treated cells to be able to combine the different independent experiments.

Recombinant HepaRG cells lines

HepaRG-Cas9 KO cell lines were generated using lentivirus co-expressing codon-optimized Cas9 nuclease along with a single guide RNA (sgRNA) targeting a particular gene (e.g., TLR1, 2, 3, etc.). LentiCRISPR plasmid contains hSpCas9 and the chimeric guide RNA cloned into a *BsmB*I site as a pair of annealed primers. The primers, designed based on the target site sequence, are flanked on the 3' end by a PAM sequence (NGG). Two sequences (called G1 and G2) for sgRNA TLR1, TLR2, TLR3 and MyD88 were designed for lentiCRISPR plasmid construction (listed in ***supplementary material and method***). Lentiviral production was classically performed in HEK293T, lentiCRISPR were cotransfected with packaging plasmids pVSVg and Gag Pol. Five days post transfection, supernatants were recovered, filtered and concentrated. Lentiviruses were then transduced in proliferative HepaRG cells

and polyclonal lines were obtained by antibiotic selection. The selection of lines was done according to KO revealed in western blot.

Viability/cytotoxicity assays

Neutral red uptake assays were performed to estimate cell viability/cytotoxicity as previously described [17]. CellTiter-Glo® Luminescent Viability Assay (Promega) was performed according to manufacturer's recommendations.

Nucleic acid extractions, reverse transcription and qPCR analyses

Total intracellular RNA and DNA were extracted from cells with the NucleoSpin RNA II kit and tissue kit respectively according to the manufacturer's instructions (Macherey-Nagel). For cccDNA analyses, total DNA was extracted using MasterPure™ DNA and RNA Purification Kit (Epicentre) in the absence of the serine protease, Proteinase K. Indeed, as viral polymerase is linked to cccDNA, the step of protein precipitation allowed us to get rid of rcDNA contamination. The next steps were realized according to manufacturer's recommendations before being quantified by qPCR. RcDNA from HBV particles was isolated from the cell supernatants using the NucleoSpin RNA Virus kit (Macherey-Nagel) according to the manufacturer's instructions.

RNA reverse transcription was performed using the Maxima RT as instructed by provider (Life Technologies). Quantitative PCR for HBV were performed using specific primers and normalized to *PRNP/RPLP0* housekeeping gene as previously described [13].

CccDNA was quantified using a FRET-based qPCR approach. Taqman™ Master Mix (ThermoFisher) was used according to manufacturer's recommendations, in presence of specific primers and cccDNA probe (c.f. to [13, 23] for details).

ELISA and CLIA

Secreted antigens HBeAg and HBsAg were detected in the supernatant of HBV-infected cells using CLIA Autobio kits, according to manufacturer's instructions (AutoBio, China). Human IL-6 and human IL-10 cytokines were detected in the supernatants using the DuoSet® ELISA kit according to the manufacturer (R&D Systems). ELISA plates were analyzed using Luminoskan™ (ThermoFisher) or Multiskan EX (ThermoFisher).

Western blot analyses

Cells were harvested in RIPA lysis buffer (NaCl 150mM, Tris HCL pH=8.0 50 mM, SDS 0.1%, NP40 1%, Na Deoxycholate 0.5%) containing protease inhibitors (Protein Cocktail Inhibitors from Sigma-Aldrich) and phosphatase inhibitors (Pierce™ Phosphatase Inhibitor Mini Tablets from ThermoFisher). Clarified lysates were then subjected to 10% SDS-PAGE using precast protein gels (Novex Wedge well 4-20% or 10% Tris-glycine gels from ThermoFisher) and separated proteins transferred onto nitrocellulose membranes using the iBlot2 apparatus according to the manufacturer (Thermofisher Scientific). Membranes were then blocked in 1X Tris-Buffered Saline, containing 0.1% of tween (TBS-T) and 5% BSA (Bovine Serum Albumin). Primary antibodies (listed in supplementary material and methods) were incubated overnight at 4°C, at concentrations indicated by the supplier. After being washed, membranes were incubated with corresponding secondary HRP antibodies for one hour. Membranes were incubated with chimioluminescent substrate SuperSignal™ according to manufacturer's recommendations (ThermoFisher) after being revealed using Gel Doc™ XR+ Imager (Biorad).

RNA sequencing and analyses

RNAs were extracted with the miRNeasy Kit (Qiagen) according to the manufacturer's instruction. Library preparation for bulk 3'-sequencing of poly(A)-RNA was done as described previously [24]. The library was sequenced on a NextSeq 500 (Illumina) with 65 cycles for the cDNA in read1 and 16 cycles

for the barcodes and UMIs in read2. Gencode gene annotations v28 and the human reference genome GRCh38 were derived from the Gencode homepage (EMBL-EBI). Dropseq tool v1.12 [25] was used for mapping raw sequencing data to the reference genome. The resulting UMI filtered count matrix was imported into R v3.4.4. CPM (counts per million) values were calculated for the raw data and genes having a mean cpm value less than 1 were removed from the dataset. Prior differential expression analysis with DESeq2 v1.18.1 (10.1186/s13059-014-0550-8), dispersion of the data was estimated with a parametric fit using a dummy variable that codes all treatment-genotype combinations. The Wald test was used for determining differentially regulated genes between all treatments within a given genotype, as well as between genotypes for a particular treatment. Shrunken log2 fold changes were calculated afterwards. A gene was determined to be differentially regulated if the absolute apeglm shrunken log2 fold change was at least 1 and the adjusted p-value was below 0.01. GSEA v4.0.3 (https://doi.org/10.1073/pnas.0506580102) was performed in the pre-ranked mode, where the fold change was used as ranking metric. All genes for which a test was conducted went into the analysis. Reference gene sets from the MsigDB v7.1 (https://doi.org/10.1093/bioinformatics/btr260) where used for testing. A pathway was considered to be significantly associated with a genotype if the FDR value was below 0.05. Rlog transformation of the data was performed for visualization and further downstream analysis. Raw sequencing data are available under the accession number PRJEB39477.

Statistic analyses

Results were expressed as means and standard deviation (SD). Statistics were performed using GraphPad software. Mann-Whitney and two-paired t- tests were mainly used to compare treatment groups. For all tests, a p value ≤ 0.05 was considered as significant. * corresponds to p value ≤ 0.05; ** corresponds to p value ≤ 0.005; *** corresponds to p value ≤ 0.001.

Results

Broadness, selectivity, and pathway specificity of Pam3CSK4-induced inhibitory phenotypes. We first confirmed that Pam3CSK4 was capable to inhibit HBV (genotype D) replication in dHepaRG cells. The levels of all HBV parameters analyzed, (including intracellular total HBV RNAs, viremia, and secretion of viral antigens) were significantly reduced even at very low concentration of Pam3CSK4 (**Fig. Sup. 1A**). Interestingly Pam3CSK4 was also capable to inhibit the replication of another HBV genotype (genotype C) (**Fig. Sup. 1B**), thus suggesting a broad antiviral activity against HBV.

The anti-HBV activity of Pam3CSK4 was not due to any cellular toxicity, as no decline of the capacity of neutral red lysosomal storage or ATP synthesis was observed even at the highest concentration tested (24,000 ng/mL) in both HepRG cells and primary human hepatocytes (**Fig. Sup. 2A**); this emphasized a very high selectivity index (SI) of the Pam3CSK4 antiviral action (i.e. ratio tox/activity at a given concentration; SI >1600). Despite this lack of toxicity, a significant decline of HNF4α expression at mRNA level was noticed even at rather low concentration (30 ng/mL) of Pam3CSK4 (**Fig. Sup. 2B**), suggesting that a dedifferentiation of cells could also account for the antiviral effect observed. However, at 15ng/mL of Pam3CSK4, which already leads to a 50% reduction of intracellular HBV RNA accumulation (**Fig. Sup. 1A**), the reduction of HNF4α mRNA was not significant (**Fig. Sup. 2B**); this was further confirmed at protein level (**Fig. Sup. 2C**), evidencing a window of antiviral activity independent of any potential loss of hepatocyte differentiation. It is important to note that the Pam3CSK4-induced decrease in HNF4α mRNA expression was reversible, as an arrest in treatment was associated to a return to baseline expression within 14 days off-drug (**Fig. Sup. 2D**); moreover all other immune-stimulators tested (*i.e.* IFNα and LTβR agonist [20]) were also associated with a transient decrease in HNF4α mRNA expression, thus suggesting a "class effect" more than a specific profile of Pam3CSK4. Altogether if the reduction of HNF4α expression might be part of the mode of action of the antiviral effect observed, it is unlikely that it represents a significative toxicologic component.

Having confirmed the broadness and selectivity of action of Pam3CSK4, we asked the question of its specificity. Pam3CSK4 is a well-characterized and specific TLR1/2 ligand. To determine whether the anti-HBV action of Pam4CSK4 in our HBV-infected hepatocytes was dependent on TLR1/2 and its adaptor MyD88, we used various knocked-out (KO) recombinant HepaRG cell lines obtained by CRISPR-Cas9 technology. Three cell lines respectively KO for TLR1, TLR2, MyD88, plus a control cell line designed to KO TLR3, were generated and validated for their KO phenotypes (**Fig. Sup. 3**). The anti-HBV activity of Pam3CSK4 was lost on all HBV parameters studied in TLR1, TLR2, and MyD88 KO cells, whereas it was conserved in the irrelevant TLR3 KO cell line (**Fig. 1**). The antiviral activity of other anti-HBV drugs, including IFNα, a nucleoside analogue (3TC/lamivudine), and an HBV RNA destabilizer (RG7834) remained similar in all cell lines, thus further validating the relevance of these cell lines for working out the TLR1/2-MyD88 specificity of action of Pam3CSK4. Interestingly a partial invalidation of the TLR2 expression (**Fig. 2A and 2B**), obtained by a more conventional RNA interference strategy (as opposed to the efficient CRISPR-Cas9 strategy described above), did not abrogate the Pam3CSK4 antiviral activity (**Fig. 2C**), thus suggesting that a low functional level of TLR2 is sufficient for the therapeutic benefit of Pam3CSK4. This is highly relevant, as a decreased expression of TLR2 was reported in both hepatocytes and liver myeloid cells in CHB patients [26]. Interestingly, targeting TLR1 or TLR6 with specific siRNA do affect the feed-forward expression of TLR2 in the context of Pam3CSK4 activation (**Fig. 2B**); but only invalidation of TLR1 led to a reduced inhibitory effect of Pam3CSK4 (**Fig. 2C**; comparison of groups of bars of siCtrl versus siTLR1), thus confirming that Pam3CSK4 likely signals through TLR1/2 heterodimers in hepatocytes. Finally, it is worth noting that the respective siRNA invalidation of TLR1, 2, or 6, as well as of MyD88, did not affect the basal replication of HBV in the absence of treatment with Pam3CSK4 (**Fig. Sup. 4**), thus consolidating the previous observations.

As expected and described in literature, Pam3CSK4 induced a rapid activation of the canonical NF-κB pathway, as measured by the phosphorylation of the p65 subunit (pp65) detectable already 30 minutes post-treatment, which remained detectable until 2 hours post-treatment (**Fig. Sup. 5**). The

turn-over was very fast with a return to baseline of pp65 level by 4 hours post treatment. No obvious activation of the non-canonical pathway was evidenced, with no increase of p52 levels observed.

Kinetics of events, priority of action on HBV RNA vs cccDNA, and long-lasting character of inhibitory phenotypes.

In our previous study, a Pam3CSK4-induced reduction of cccDNA level was observed in both HBV-infected dHepaRG and PHH [13]. As cccDNA is the nuclear episomal template responsible for persistence and biogenesis of all downstream HBV replication intermediates and antigens, we aimed at investigating whether the effect of Pam3CSK4 on HBV RNA accumulation could be either independent or prior to any decline on cccDNA. At the lowest dose of Pam3CSK4 (10 ng/mL), a decline of HBV RNAs was observed in absence of any significant decline of cccDNA level (**Fig. 3A**), thus defining treatment condition able to somehow disconnect both inhibitory phenotypes. At 100 ng/mL, a concomitant and similar inhibition of HBV RNA and cccDNA accumulation was observed; this concentration will be mainly used in the rest of the study. We further investigated whether the inhibitory effect on HBV RNA accumulation could come faster than that on cccDNA. HBV-infected cells were treated only once and levels of intracellular HBV RNAs and cccDNA, as well as secreted HBV antigens, were monitored in short-term kinetic experiments (**Fig. 3B**). The inhibitory effect on HBV RNA level was first to occur, leading to a 70% reduction at 48 hours post-treatment, whereas cccDNA level remained stable in this short-term kinetic analysis. It is also worth noting that this fast Pam3CSK4-induced decline of HBV RNAs translated into a quasi-concomitant reduction of HBeAg secretion, whereas HBsAg remained unchanged. Finally, we shortened the timing of analyses in order to analyze the detailed kinetic of HBV RNA decline; the quantification of total versus pgRNA was performed (**Fig. 3C**). Altogether, this result indicates that Pam3CSK4 acts first on HBV RNAs, and in particular on pgRNA, before acting on cccDNA level that is likely secondarily involved in a long-term

sustained phenotype on HBV RNA levels. A particular investigation of the effect of Pam4SCK4 on RNA biogenesis/accumulation will follow.

As Pam3CSK4 has an effect on both cccDNA and HBV RNA levels, we wondered whether a long-lasting inhibition after treatment arrest could be obtained with this ligand. To this end, persistently HBV-infected dHepaRG cells, treated as in previous experiments, were kept in culture 10 days after the end of treatment to monitor potential rebound of HBV parameters. IFN-α, RG7834 (HBV RNAs destabilizer) and Tenofovir (TFV; a NA) were used as controls. As seen before, Pam3CSK4 induced a strong decrease of all HBV parameters at the end of treatment (**Fig. 4**). Interestingly, it is the only drug to induce a strong decrease of cccDNA right after treatment (**Fig. 4A**), while IFN-α, a drug currently used in clinic, does not have any impact on cccDNA at the end of treatment. In contrast to the expected ongoing rebound of viremia observed with TFV (**Fig. 4E and Fig. Sup. 6**) and rebound of both HBV RNAs and secreted antigens observed with RG7834 (**Fig. 4B-D and Fig. Sup. 6**), the reduction of all HBV parameters was sustained with Pam3CSK4, as well as with IFN-α, the other innate immune stimulator used as control here (**Fig. 4**). The phenotype observed regarding cccDNA inhibition by Pam3CSK4 and IFN-α, whereas both drugs inhibit strongly and durably all other HBV parameters, might suggest different MoAs for these innate immune stimulators; i.e. “silencing” for IFN-α versus likely “silencing + strong degradation” for Pam3CSK4.

***Pam3CSK4 both reduced the level of nascent HBV RNAs and accelerated HBV RNA decay*.**

The antiviral activity of Pam3CSK4 on HBV RNAs biogenesis/accumulation was further analyzed, as it is one of the most important inhibitory phenotype induced by this innate immune stimulator. We first investigated, using dHepaRG, the ability of Pam3CSK4 to inhibit HBV transcription by Run-On experiments (measurement by specific RT-qPCR to detect HBV RNAs that incorporated 5-ethynyl uridine (EU) after a pulse of 2h). As a control, infected but not treated cells were incubated with actinomycin D, an inhibitor of RNA polymerase II, 20 minutes before adding EU. Moreover RG7834

(HBV RNAs destabilizer), which acts only on RNA-decay and not on RNA transcription [27, 28], as well as IFN-α, which act at both levels, were also used to benchmark Pam3CSK4 activity. Before incorporation of labeled ribonucleoside, the anti-HBV effect of all molecules on secreted parameters was monitored (**Fig. 5A; and Fig. Sup. 6** for kinetic analyses on secreted parameters). After labeling, total intracellular HBV RNAs were isolated and first quantified by RT-qPCR. Labeled RNAs were further extracted using Click-iT™ Nascent RNA Capture Kit, and quantified by RT-qPCR (**Fig. 5B**). Pam3CSK4 was the most active at reducing the level of nascent HBV RNAs, in addition to total RNA level, thus suggesting an effect on cccDNA transcription. IFN-α, which was already described as a modulator of HBV transcription [29], induced also a reduction of both RNA levels, whereas other controls behaved as expected. Of note, it is acknowledged that 2h of labeling is too long for a *bona fide* Run-On analysis, but shorter time did not allow generating analyzable results (***data not shown***). Hence, we could not exclude the fact that Pam3CSK4 could also induce RNA degradation.

To test this hypothesis, we performed RNA decay analyses in both HBV-infected dHepaRG and PHH cells treated with the same drugs (at indicated respective concentrations). To stop transcription and analyze RNA decay over a period of 24h, tripolide was added to cell culture media two days after the last treatment with drugs. HBV RNA levels were checked before tripolide treatment to insure that drugs worked; it is worth noting that a single treatment with IFN-α did not lead to a strong inhibitory phenotype (**Fig. 5C**). RNAs were then extracted at different time points post-triptolide treatment. PRNP mRNA, a housekeeping gene, and HNF4-α mRNA, whose half-life is short, were respectively used as negative and positive controls (**Fig. Sup. 7**). Pam3CSK4 induced a rapid degradation of viral RNAs after only one treatment in both models (**Fig. 5D**). It was the most efficient at inducing HBV RNA degradation in dHepaRG, whereas it was slightly less efficient than controls in PHH. This is likely due to the fact that TLR2 is already well expressed at baseline in dHepaRG but need to be induced by Pam3CSK4 in PHH; therefore a single treatment in PHH is less efficient and multiple treatment tend to improve efficacy over time in a feed-forward loop manner.

***Searching for Pam3CSK4-induced host effectors that could be responsible for RNA and cccDNA declines*.**

Many data are available regarding the modulation of host gene expression by the TLR2/Myd88/NF-κB axis. However, in order to analyze genes modulated by Pam3CSK4 in our model, we performed RNA-sequencing of RNAs extracted 48 hours post-treatment from either mock or infected dHepaRG cells. Differentially analyzed and important biological signatures modulated by Pam3CSK4 were obtained comparing the list of gene generated by MSigDB (Molecular Signature Database) in the GSEA (Gene set enrichment analysis) software. As expected, Pam3CSK4 induced numerous immune pathways, NF-κB pathway being the most induced, in mock and infected conditions, with respectively 73 and 74 significantly modulated genes with an enrichment score of at least 2.5 (**Fig. Sup. 8**). This strong induction of NF-κB pathway was linked to strong IL-6/JAK/STAT3 responses in either auto or paracrine manner, with respectively 34 and 30 genes up regulated in mock and infected conditions. In contrast, and as seen before, Pam3CSK4 inhibited numerous metabolic mechanisms, including oxidative phosphorylation, bile acid and fatty acid metabolisms.

To get further insight on cellular mechanisms modified by Pam3CSK4, genes modulated by Pam3CSK4 were modeled using Cytoscape software to highlight those that can be responsible of both the decrease of viral HBV RNA and cccDNA levels observed *in vitro*. A preliminary analysis using GSEA software using database referenced by Reimand and colleagues [30], which regrouped known biological processes and pathways allowed the identification of diverse mechanisms induced by Pam3CSK4 (**Fig. Sup. 9**). As expected, Pam3CSK4 induced a strong immune response with among others the up regulation of effectors responsible for the regulation of innate immune response, PRR and IL-6 pathways, as well as NF-κB signaling. Interestingly, we found that Pam3CSK4 modulated genes involved in RNA metabolism. MCPIP1 (also called ZC3H12A or Regnase-1) and RNAseH2 were the two top genes found up regulated in the RNA catabolism cluster, with Log2FC (Rank) of 2.7 and

1.22 respectively; they both have RNAse properties. MCPIP1 was recently shown to restrict HBV replication by targeting terminal redundancies sequences of HBV RNA in overexpression conditions [31, 32], and represented therefore a good effector candidate to explain the effect on HBV RNA induced by Pam3CSK4. Pam3CSK4 also slightly induced Flap endonuclease 1 (FEN-1), which possesses 5'-flap endonuclease and 5'-3' exonuclease activities and is involved in DNA replication and repair. FEN-1 was recently shown being involved in cccDNA formation [33, 34]; moreover a functional link between FEN-1 and RNAseH was recently disclosed [35]. We therefore performed loss of function experiments of these hits (MCPIP1, RNAseH2 and FEN-1) and analyzed if the antiviral activity of Pam3CSK4 was reversed.

Focusing first on effector candidates with RNAse activities, we used siRNA against MCPIP1 and RNAseH2 to determine whether we could revert Pam3CSK4 anti-HBV activities. As shown in **Fig. Sup. 10A**, no reversion of Pam3CSK4 effect was observed when RNAseH2 was successfully silenced. Despite many attempts, the siRNA strategy failed to decrease MCPIP1 expression (***data not shown***); therefore we used a CRISPR-Cas9 engineered HepaRG cell line to investigate the potential role of MCPIP1 in Pam3CSK4-induced anti-HBV effect. Two distinct MCPIP1-KO cell lines were generated with two different RNA guides, and the invalidation was monitored by western blotting (**Fig. Sup. 10B**). As shown in **Fig. Sup. 10C**, no reversion of Pam3CSK4 effect was observed in MCPIP1-KO cells. Altogether, this indicates that the effect of Pam3CSK4 on HBV RNA accumulation is not due to the up regulation of the expression of these two RNAses tested. As no other genes with RNAse activity were found in the list of up-regulated genes coming from the RNA-seq analysis, we tested whether the neo-synthesis/neo-production of a host effector was necessary for the Pam3CSK4 effect on HBV RNA accumulation. To this end, infected dHepaRG cells were simultaneously treated by Pam3CSK4 and cycloheximide (CHX), an inhibitor of translation/protein synthesis, and the effect on HBV RNA was quantified by RT-qPCR. HNF4α mRNA level was used as control, as IL-6 induced by Pam3CSK4 treatment was previously shown to be responsible for the degradation of HNF4-α transcripts [36].

Interestingly, we did not observe significant changes in HBV RNA accumulation in both conditions (with and without CHX; slopes are similar), whereas, as expected, the presence of CHX changed completely the profile of HNF4α RNA accumulation (**Fig. Sup. 11**). This result indicates that the Pam3CSK4-induced inhibitory effect on HBV RNA might be due to a post-translational event on a host-effector or a host-pathway.

Next, we wanted to get advanced on the identification of a host effector (induced by Pam3SCK4 and in the list of the RNA-seq analysis) involved in the degradation of cccDNA. As APOBEC3B was previously identified as involved in cccDNA degradation induced by a lymphotoxin-beta receptor agonist (BS1, a monoclonal Ab) [20], we checked whether this factor could be involved in Pam3SCK4 inhibitory phenotypes using RNA interference. No changes were observed in the patterns of Pam3CSK4 inhibition (**Fig. Sup. 12**), thus ruling-out any implication of APOBEC3B. We next tested the Flap endonuclease 1, which was one of the top lister of the RNA seq analysis and was recently reported to be involved in cccDNA post-HBV-entry biogenesis [33, 34]. A loss-of-function on FEN-1, obtained by RNA interference (**Fig. Sup. 13**), allowed a significant reversion of the Pam3CSK4 inhibitory phenotype on cccDNA and HBV RNAs, thus suggesting that this effector might contribute in the loss of cccDNA induced by Pam3CSK4. However, the reversion was only partial and other effectors might be involved and remain to be identified.

***Effect of Pam3CSK4 in combination with approved or investigational anti-HBV drugs*.**

As stated in the introductory section current treatments mainly administrated as monotherapies are not capable to cure HBV infections. There is a consensus upon the fact that combinations are to be clinically tested to identify the best one to improve HBV cure rates [3, 4]. We therefore tested in mono or combination settings the anti-HBV efficacy of various drugs, including Pam3CSK4, IFNα, tenofovir (TFV), type I and II CAMs, previously tested by Lahlali and colleagues [19], the FXR agonist GW4064, used as a prototypic anti-HBV asset in this class of drug [37, 38], and 1C8 a kinase inhibitor with anti-

HBV activity reported in [39]. Low concentrations of the different assets were used to evidence additional inhibitory effect on HBV parameters. In side-by-side comparison and mono-therapy, Pam3CSK4 was the best anti-HBV asset (**Fig. 6**). Its combination with IFNα and the kinase inhibitor 1C8 led to improved antiviral activity in the absence of any toxicity (under microscope and in terms of RNA extraction yield), and, surprisingly, the best effect on cccDNA and HBsAg secretion was obtained with Pam3CSK4 + 1C8. It is worth noting that this combination led also to the highest impact on HNF4a expression, as monitored by RT-qPCR. Triple combinations did not lead to better anti-HBV effect and were associated with higher cell toxicity and they were not considered further.

Next, we evaluated the long-lasting effect of mono and dual therapies to determine whether the long-lasting effect, induced by Pam3CSK4 in monotherapy (**Fig. 4**), would be modulated by the other drugs. We added in the list of drug tested RG7834, as this one in monotherapy is associated with a rebound on HBV RNA off treatment and represented a good control. No antagonistic effect of other drugs on Pam3CSK4-induced effect on cccDNA or HBV RNA levels was noticed and the improvements seen with Pam3CSK4 + IFNα and Pam3CSK4 + KINi combos were confirmed (**Fig. Sup. 14**). Altogether these results set the landscape for *in vivo* evaluation of a combination therapy including Pam3CSK4.

Discussion

Peg-IFNα remains in many countries, even very industrialized, a clinically used drug to fight chronic HBV (and HDV) infections (CHB) in patients despite its poor tolerability [3, 4]. Its advantage over nucleoside analogues, which are mainly used to get HBV viro-suppression, is that it is administrated for no more than 48 weeks (*i.e.* finite duration regimen) and it leads to a higher rate of HBsAg loss, which is viewed as a good marker of functional HBV cure [1]. Yet, efforts to replace this innate immune cytokine by other innate immune stimulators are important [10]; hence, TLR7, TLR8 and RIGI/NOD2 agonists have been recently evaluated in clinical trials in CHB patients. If the latter was stopped because of toxicity, the two first types of agonists did not show great antiviral effect in monotherapies [40, 41]. Echoing this, TLR7 and TLR8 agonists were not capable to directly inhibit *in vitro* HBV replication in immune competent hepatocyte, mainly because human hepatocytes do not express functional TLR7 and 8 [13, 16, 18]. In contrast, TLR2 agonist and in particular Pam3CSK4 was shown to be second best efficient (the riboxxol TLR3 agonist was more potent) at directly inhibiting HBV replication within hepatocytes [13].

In this study, performed exclusively *in vitro*, we investigated the anti-HBV mode of action of Pam3CSK4 in physiologically relevant human hepatocytes (both HepaRG cells and PHH). We confirmed its potency, uncovered its selectivity in absence of any toxicity, suggested its pan-genotypic activity, and verified it specificity. Regarding the latter point, we indeed demonstrated, for the first time in human hepatocytes, that Pam3CSK4 mediates its anti-HBV effect in a TLR1/2-Myd88-dependent manner via the activation of the NF-κB canonical pathway. We have also shown that a very low level of TLR2 expression is necessary and sufficient to obtain the anti-HBV inhibitory effect. This is an important observation as a reduction of TLR2 expression in both hepatocytes and myeloid cells in CHB patients was previously reported [26]. The fact that such a reduction is induced by HBV *in vivo* and that HBV is very sensitive to TLR2 agonisation makes sense, as pathogens tend to counteract host factor functions harmful for them.

Future therapy against HBV would have to be long-lasting, meaning that the antiviral effect should persist off treatment. This could be achieved by restoration of specific immune responses and we will not discuss further this immunological component here. But it has to be associated with a decreased activity of cccDNA, which is the main template for the biogenesis of all downstream HBV replication intermediates. A modulation of cccDNA activity has been very recently confirmed in the natural history of HBV infection, leading to a progressive reduction of viral replication [42]. A therapeutic decreased activity of cccDNA can theoretically be obtained by either degradation/loss of cccDNA or defunctionalization/silencing; both would lead to a reduction of HBV RNA biogenesis, including the longest transcript, the pregenomic RNA, pgRNA. Here we have confirmed that Pam3CSK4 is capable to induce a strong reduction of HBV RNA levels, which originates from both a decrease in cccDNA amount and transcriptional activity, but we have shown that these phenotypes are also accompanied by an acceleration of RNA decay/degradation. In terms of kinetics of event, Pam3CSK4 induces first a reduction of RNA levels in the absence of any change in cccDNA amount; then a decrease of cccDNA level complete this step-by step established inhibitory phenotype. This MoA is slightly different than that obtained with very high doses of IFNα in our models; IFNα does also induce a strong reduction of HBV RNA levels, but the impact on the amount of cccDNA is less significant. Pam3SCK4 has a similar effect than LT-βR agonist [20], except that the mediation of its antiviral effect involves only the canonical NF-κB pathway.

Functional analyses were performed, following the acquisition of RNA sequencing data in our models, to identify host factors involved in the two main inhibitory phenotypes, which are acceleration of HBV RNA decay and degradation/loss of cccDNA. The two hits from our RNA seq data, bearing RNAse activities, namely RNAseH2 and MCPIP1 were rule-out, by loss of function studies, to be involved in the Pam3CSK4-induced RNA decay. Further analyses will be necessary to identify the main host factor involved in this phenotype. We have generated preliminary data suggesting that the factor involved might be regulated at post-translational levels, as the use of the translation inhibitor cycloheximide

did not change the slope of the Pam3CSK4-induced RNA decay. For the loss of cccDNA amount, we have shown that its was independent of APOBEC3B, which was identified as the main host factor involved in LT-βR agonist-induced cccDNA degradation [20]. Interestingly, we found that flap endonuclease 1 (FEN-1), a host factor recently confirmed as important for the conversion of rcDNA into cccDNA upon neo-infection/neo-entry of HBV into cells [34], contribute to the Pam3CSK4-induced inhibitory phenotype on cccDNA. This suggests that FEN-1 may be involved, together with other host factor yet to be identified, in the regulation of the level of cccDNA when its level is already established, and that a therapeutic increase of FEN-1 could accelerate cccDNA decline. Our finding warrants therapeutic investigation based on the overexpression of FEN-1 in HBV-infected hepatocytes using AAV vectors for instance. It is worth noting that FEN-1 is physiologically involved in host DNA repair, DNA replication, and genome stability, and has recently been identified as an interesting target in oncology [43, 44]. If FEN-1 contributes to the Pam3CSK4-induced inhibitory effect on cccDNA level, it is likely not the sole host-factor involved, as the reversion of the phenotype in loss of function study was not complete. Further studies are required to identify novel host-factor, other than APOBEC3B and FEN-1, involved in cccDNA amount regulation during natural history as well as in the frame of a therapeutic intervention.

As Pam3CSK4 induces, through the activation of TLR1/2-MyD88 pathway, a strong decline of HBV RNA and cccDNA levels, it was not a surprise to found that it leads to a durable antiviral effect, with no rebound observed off treatment. This long-lasting effect is a strong advantage for a molecule in the perspective of HBV cure. Here we also combined Pam3SCK4 with other anti-HBV molecules, either approved or investigational drugs, in order to pave the way for novel therapeutic strategies. Interestingly, we found that combinations of Pam3CSK4 with either IFNα or the kinase inhibitor 1C8 (described in [39]) lead to improved inhibitory phenotypes. In particular, the level of cccDNA was further decreased in combinations arms. As mono-therapies with either IFNα or 1C8 did not have any effect on cccDNA (at the concentration used in these combinations studies in differentiated HepaRG

cells), it is likely that these improvements are synergistic. Further experiments should be performed in PHH or in liver humanized mice to confirm this. Moreover, the synergistic character of the combination Pam3CSK4 and the kinase inhibitor, warrant further investigation as it could reveal a novel role of the kinase targeted by 1C8 in cccDNA biology. Cytotoxicity studies are also to be carefully performed to establish the safety of such combinations.

TLR2 agonisation to achieve an anti-HBV inhibitory phenotype *in vivo* seems to be an interesting therapeutic option. Indeed here, we have shown that a TLR2 agonist can directly inhibit HBV replication in hepatocytes, but one should not forget that TLR2 agonist could also foster liver macrophages into a pro-inflammatory and antiviral process. Recently, we have shown that liver macrophages were twisted towards an immune tolerant M2-like phenotype in CHB patients, which is favorable to the persistence of HBV replication [45]. TLR2 agonisation in these M2 macrophages is likely to revert their phenotypes into M1-like ones, which are more prone to viral elimination. We are currently testing this hypothesis in AAV-HBV transduced mice. For this purpose polylacticacid (PLA) nanoparticles containing Pam3CSK4 were generated [46]. This nanoparticulation is necessary to protect the TLR2 agonist and allow delivery to the liver upon intravenous injection.

Acknowledgements

The authors would like to thank Jennifer Molle and Anaëlle Dubois for their help for the isolation of primary human hepatocytes, as well as Prof Michel Rivoire (CLB and INSERM U1032), and his staff from the surgery room, for providing us with liver resections.

References

[1] EASL 2017 Clinical Practice Guidelines on the management of hepatitis B virus infection. Journal of hepatology 2017;67:370-398.

[2] Chan SL, Wong VW, Qin S, Chan HL. Infection and Cancer: The Case of Hepatitis B. Journal of clinical oncology : official journal of the American Society of Clinical Oncology 2016;34:83-90.

[3] Durantel D, Zoulim F. New antiviral targets for innovative treatment concepts for hepatitis B virus and hepatitis delta virus. Journal of hepatology 2016;64:S117-131.

[4] Fanning GC, Zoulim F, Hou J, Bertoletti A. Therapeutic strategies for hepatitis B virus infection: towards a cure. Nat Rev Drug Discov 2019;18:827-844.

[5] Viganò M, Grossi G, Loglio A, Lampertico P. Treatment of hepatitis B: Is there still a role for interferon? 2018;38 Suppl 1:79-83.

[6] Abdrakhman A, Ashimkhanova A, Almawi WY. Effectiveness of pegylated interferon monotherapy in the treatment of chronic hepatitis D virus infection: A meta-analysis. Antiviral research 2021;185:104995.

[7] Bazinet M, Pantea V, Cebotarescu V, Cojuhari L, Jimbei P, Albrecht J, et al. Safety and efficacy of REP 2139 and pegylated interferon alfa-2a for treatment-naive patients with chronic hepatitis B virus and hepatitis D virus co-infection (REP 301 and REP 301-LTF): a non-randomised, open-label, phase 2 trial. The lancet Gastroenterology & hepatology 2017;2:877-889.

[8] Bazinet M, Pantea V, Placinta G, Moscalu I, Cebotarescu V, Cojuhari L, et al. Safety and Efficacy of 48 Weeks REP 2139 or REP 2165, Tenofovir Disoproxil, and Pegylated Interferon Alfa-2a in Patients With Chronic HBV Infection Naive to Nucleos(t)ide Therapy. Gastroenterology 2020.

[9] Bogomolov P, Alexandrov A, Voronkova N, Macievich M, Kokina K, Petrachenkova M, et al. Treatment of chronic hepatitis D with the entry inhibitor myrcludex B: First results of a phase Ib/IIa study. Journal of hepatology 2016;65:490-498.

[10] Gehring AJ, Protzer U. Targeting Innate and Adaptive Immune Responses to Cure Chronic HBV Infection. Gastroenterology 2019;156:325-337.

[11] Isorce N, Lucifora J, Zoulim F, Durantel D. Immune-modulators to combat hepatitis B virus infection: From IFN-alpha to novel investigational immunotherapeutic strategies. Antiviral research 2015;122:69-81.

[12] Isogawa M, Robek MD, Furuichi Y, Chisari FV. Toll-like receptor signaling inhibits hepatitis B virus replication in vivo. Journal of virology 2005;79:7269-7272.

[13] Lucifora J, Bonnin M, Aillot L, Fusil F, Maadadi S, Dimier L, et al. Direct antiviral properties of TLR ligands against HBV replication in immune-competent hepatocytes. Scientific reports 2018;8:5390.

[14] Gripon P, Rumin S, Urban S, Le Seyec J, Glaise D, Cannie I, et al. Infection of a human hepatoma cell line by hepatitis B virus. Proc Natl Acad Sci U S A 2002;99:15655-15660.

[15] Lecluyse EL, Alexandre E. Isolation and culture of primary hepatocytes from resected human liver tissue. Methods in molecular biology (Clifton, NJ) 2010;640:57-82.

[16] Faure-Dupuy S, Vegna S, Aillot L, Dimier L, Esser K, Broxtermann M, et al. Characterization of Pattern Recognition Receptor Expression and Functionality in Liver Primary Cells and Derived Cell Lines. Journal of innate immunity 2018;10:339-348.

[17] Isorce N, Testoni B, Locatelli M, Fresquet J, Rivoire M, Luangsay S, et al. Antiviral activity of various interferons and pro-inflammatory cytokines in non-transformed cultured hepatocytes infected with hepatitis B virus. Antiviral research 2016;130:36-45.

[18] Luangsay S, Ait-Goughoulte M, Michelet M, Floriot O, Bonnin M, Gruffaz M, et al. Expression and functionality of Toll- and RIG-like receptors in HepaRG cells. Journal of hepatology 2015;63:1077-1085.

[19] Lahlali T, Berke JM, Vergauwen K, Foca A, Vandyck K, Pauwels F, et al. Novel potent capsid assembly modulators regulate multiple steps of the Hepatitis B virus life-cycle. Antimicrobial agents and chemotherapy 2018.

[20] Lucifora J, Xia Y, Reisinger F, Zhang K, Stadler D, Cheng X. Specific and nonhepatotoxic degradation of nuclear hepatitis B virus cccDNA. Science 2014;343:1221-1228.

[21] Lucifora J, Michelet M, Rivoire M, Protzer U, Durantel D, Zoulim F. Two-dimensional-cultures of primary human hepatocytes allow efficient HBV infection: Old tricks still work! Journal of hepatology 2020;73:449-451.

[22] Ladner SK, Otto MJ, Barker CS, Zaifert K, Wang GH, Guo JT, et al. Inducible expression of human hepatitis B virus (HBV) in stably transfected hepatoblastoma cells: a novel system for screening potential inhibitors of HBV replication. Antimicrobial agents and chemotherapy 1997;41:1715-1720.

[23] Lucifora J, Salvetti A, Marniquet X, Mailly L, Testoni B, Fusil F, et al. Detection of the hepatitis B virus (HBV) covalently-closed-circular DNA (cccDNA) in mice transduced with a recombinant AAV-HBV vector. Antiviral research 2017;145:14-19.

[24] Parekh S, Ziegenhain C, Vieth B, Enard W, Hellmann I. The impact of amplification on differential expression analyses by RNA-seq. Scientific reports 2016;6:25533.

[25] Macosko EZ, Basu A, Satija R, Nemesh J, Shekhar K, Goldman M, et al. Highly Parallel Genome-wide Expression Profiling of Individual Cells Using Nanoliter Droplets. Cell 2015;161:1202-1214.

[26] Visvanathan K, Skinner NA, Thompson AJ, Riordan SM, Sozzi V, Edwards R, et al. Regulation of Toll-like receptor-2 expression in chronic hepatitis B by the precore protein. Hepatology 2007;45:102-110.

[27] Mueller H, Lopez A, Tropberger P, Wildum S, Schmaler J, Pedersen L, et al. PAPD5/7 Are Host Factors That Are Required for Hepatitis B Virus RNA Stabilization. Hepatology 2019;69:1398-1411.

[28] Sun L, Zhang F, Guo F, Liu F, Kulsuptrakul J, Puschnik A, et al. The Dihydroquinolizinone Compound RG7834 Inhibits the Polyadenylase Function of PAPD5 and PAPD7 and Accelerates the Degradation of Matured Hepatitis B Virus Surface Protein mRNA. 2020;65.

[29] Belloni L, Allweiss L, Guerrieri F, Pediconi N, Volz T, Pollicino T, et al. IFN-alpha inhibits HBV transcription and replication in cell culture and in humanized mice by targeting the epigenetic regulation of the nuclear cccDNA minichromosome. J Clin Invest 2012;122:529-537.

[30] Reimand J, Isserlin R. Pathway enrichment analysis and visualization of omics data using g:Profiler, GSEA, Cytoscape and EnrichmentMap. 2019;14:482-517.

[31] Li M, Yang J, Zhao Y, Song Y, Yin S, Guo J, et al. MCPIP1 inhibits Hepatitis B virus replication by destabilizing viral RNA and negatively regulates the virus-induced innate inflammatory responses. Antiviral research 2020;174:104705.

[32] Li Y, Que L, Fukano K, Koura M, Kitamura K, Zheng X, et al. MCPIP1 reduces HBV-RNA by targeting its epsilon structure. Scientific reports 2020;10:20763.

[33] Kitamura K, Que L. Flap endonuclease 1 is involved in cccDNA formation in the hepatitis B virus. 2018;14:e1007124.

[34] Wei L, Ploss A. Hepatitis B virus cccDNA is formed through distinct repair processes of each strand. 2021;12:1591.

[35] Riva V, Garbelli A, Casiraghi F, Arena F, Trivisani CI, Gagliardi A, et al. Novel alternative ribonucleotide excision repair pathways in human cells by DDX3X and specialized DNA polymerases. Nucleic Acids Res 2020;48:11551-11565.

[36] Hösel M, Lucifora J, Michler T, Holz G, Gruffaz M, Stahnke S, et al. Hepatitis B virus infection enhances susceptibility toward adeno-associated viral vector transduction in vitro and in vivo. Hepatology 2014;59:2110-2120.

[37] Mouzannar K, Fusil F, Lacombe B, Ollivier A, Ménard C, Lotteau V, et al. Farnesoid X receptor-α is a proviral host factor for hepatitis B virus that is inhibited by ligands in vitro and in vivo. FASEB journal : official publication of the Federation of American Societies for Experimental Biology 2019;33:2472-2483.

[38] Radreau P, Porcherot M, Ramière C, Mouzannar K, Lotteau V, André P. Reciprocal regulation of farnesoid X receptor α activity and hepatitis B virus replication in differentiated HepaRG cells and primary human hepatocytes. FASEB journal : official publication of the Federation of American Societies for Experimental Biology 2016;30:3146-3154.

[39] Chabrolles H, Auclair H, Vegna S, Lahlali T. Hepatitis B virus Core protein nuclear interactome identifies SRSF10 as a host RNA-binding protein restricting HBV RNA production. 2020;16:e1008593.

[40] Amin OE, Colbeck EJ, Daffis S, Khan S, Ramakrishnan D, Pattabiraman D, et al. Therapeutic potential of TLR8 agonist GS-9688 (selgantolimod) in chronic hepatitis B: re-modelling of antiviral and regulatory mediators. 2020.

[41] Gane EJ, Lim YS, Gordon SC, Visvanathan K, Sicard E, Fedorak RN, et al. The oral toll-like receptor-7 agonist GS-9620 in patients with chronic hepatitis B virus infection. Journal of hepatology 2015;63:320-328.

[42] Suslov A, Meier MA, Ketterer S, Wang X, Wieland S, Heim MH. Transition to HBeAg-negative chronic hepatitis B virus infection is associated with reduced cccDNA transcriptional activity. Journal of hepatology 2021;74:794-800.

[43] Dehé PM, Gaillard PHL. Control of structure-specific endonucleases to maintain genome stability. Nature reviews Molecular cell biology 2017;18:315-330.

[44] Guo E, Ishii Y. FEN1 endonuclease as a therapeutic target for human cancers with defects in homologous recombination. 2020;117:19415-19424.

[45] Faure-Dupuy S, Delphin M, Aillot L, Dimier L, Lebosse F, Fresquet J, et al. Hepatitis B virus-induced modulation of liver macrophage function promotes hepatocyte infection. Journal of hepatology 2019;71:1086-1098.

[46] Lamrayah M, Charriaud F, Hu S, Megy S, Terreux R, Verrier B. Molecular modelling of TLR agonist Pam(3)CSK(4) entrapment in PLA nanoparticles as a tool to explain loading efficiency and functionality. International journal of pharmaceutics 2019;568:118569.

Figures legends

Figure 1. Pam3CSK4 acts through the TLR1/2-MyD88 axis to induce anti-HBV activity. Indicated differentiated HepaRG cell lines were infected with HBV with 100 vge/cell. At day-7 post-infection (p.i.), cells were treated twice with either Pam3CSK4 (100ng/mL), IFNα (500 IU/mL), RG7834 (0.1µM), or the nucleoside analogue lamivudine (3TC ; 1µM) for a total exposure time of 6 days. Cells and supernatants were harvested for analyses at day-13 post-infection. The effect on cccDNA, HBV RNAs, secreted HBV antigens, and viremia were respectively quantified by cccDNA-specific-qPCR, RT-qPCR, CLIA, and qPCR. Results are presented in percentage (%), normalized to the non-treated condition (NT). Results are the mean +/- standard deviation (SD) of one experiment, performed with three biological replicates. No statistical analysis was performed, as only one experiment was performed.

Figure 2: Low expression of TLR2 does not prevent the antiviral activity of Pam3CSK4. Differentiated HepaRG cell lines were infected with HBV with 100 vge/cell and 5 days post infection, cells were transfected once with indicated siRNAs (non-targeting = siCtrl and targeting indicated TLRs or HBV RNA). Four days post-transfection, cells were either stopped for analysis of TLR2 expression by RTqPCR (A; black bars; results normalized to housekeeping gene level and siCtrl) or mock (NT siCtrl) and treated two times with Pam3CSK4 (100ng/mL) for a total exposure time of 6 days. Then TLR2 RNAs were also quantified by RT-qPCR; results (grey bars) are expressed in percentage, normalized to housekeeping gene level and non-treated siCtrl condition (NT siCtrl). B) Effect of indicated siRNA on the expression of TLR2 assessed by western blot. C) The effect on HBV RNAs, secreted HBV antigens, and viremia were respectively quantified by RT-qPCR, CLIA, and qPCR. Results are presented in %,

normalized to the non-treated condition (NT siCtrl). Results are the mean +/- standard deviation (SD) of 3 independent experiments (n=3), performed with three biological replicates. Statistically significant differences from NT siCtrl conditions are indicated by asterisks (ns: non-significant, *P<0.05, **P<0.005, ***P<0.001). ND means not determined.

Figure 3: Pam3CSK4 induces first a decrease in HBV RNA levels, without any impact on cccDNA amount. A) Seven days post-HBV- infection, dHepaRG cells were treated twice with indicated concentrations of Pam3CSK4 (expressed in ng/mL) for a total exposure time of six days. Cells were harvested for analyses at day-13 post-infection and intracellular HBV levels of cccDNA and RNAs were quantified by FRET-qPCR method and RT-qPCR. B) Seven days post-HBV- infection, dHepaRG cells were treated once with Pam3CSK4 (100ng/mL) and cells/supernatants were harvested at the indicated times. The effect on cccDNA, HBV RNAs, and secreted HBV antigens, were respectively quantified by cccDNA-specific-qPCR, RT-qPCR, and CLIA. All results (panels A and B) are expressed in % normalized to NT or 0h conditions. Results are the mean +/- standard deviation (SD) of 3 experiments (n=3), performed with three biological replicates. Statistically significant differences from NT conditions are indicated by asterisks (ns: non-significant, *P<0.05, **P<0.005, ***P<0.001).

Figure 4. Pam3CSK4 induces a long-lasting antiviral effect. Seven days post-infection, dHepaRG were treated twice with Pam3CSK4 (100ng/mL), IFNα (500 IU/mL), RG7834 (0.1µM), Tenofovir (TFV ; 1µM) for a total exposure time of six days. HBV parameters were analyzed 14 days post-infection (at the end of treatment), and 24 days post-infection. The effect on cccDNA (A), HBV RNAs (B), secreted HBV antigens (C and D), and viremia (E) were respectively quantified by cccDNA-specific-qPCR, RT-qPCR, CLIA, and qPCR. All histograms represent the

mean of at least three independent experiments with three biological replicates and the error bars indicate SD. Statistically significant differences from NT conditions are indicated by asterisks (ns: non-significant, *P<0.05, **P<0.005, ***P<0.001).

Figure 5. Pam3CSK4 both targets HBV transcription and accelerates HBV RNA decay. A and B) Differentiated HepaRG were treated at day-7 post-infection, with Pam3CSK4 (100ng/mL), RG7834 (0.1µM), IFN-α (1000 IU/mL) and lamivudine (3TC, 1µM), for a total exposure of 6 days of treatment. Supernatants were recovered 6 days after treatment (and 13 days post-infection) and all secreted HBV parameters were quantified by CLIA and qPCR (A). At day-6 post treatment 5-ethynyl uridine was used to label nascent RNAs for two hours. HBV RNAs were then extracted and quantified by RT-qPCR for total analysis, and labelled RNAs were further extracted using Click-iT™ Nascent RNA Capture Kit according to manufacturer's recommendations, and were also quantified by RT-qPCR for total analysis (B). Actinomycin D was used as control: on day 13, cells were treated with actinomycin D at a concentration of 5µg/ml and for twenty minutes prior to the addition of 5-ethynyl uridine. All histograms represent the mean of at least three independent experiments with three biological replicates and the error bars indicate SD. Statistically significant differences from NT conditions are indicated by asterisks (ns: non-significant, *P<0.05, **P<0.005, ***P<0.001). C and D) Infected PHH or dHepaRG were treated with Pam3CSK4 (1µg/mL for PHH and 100ng/mL for dHepaRG), RG7834 (0.1 µM) and Peg-IFN-α (1000 IU/mL) for three days prior to the addition of triptolide (1µg/mL). Triptolide was added to cell medium (yet containing treatment). At indicated time, RNAs were extracted and quantified by RTqPCR with HBV primers and housekeeping genes (PRNP and HNF4α); normalization was done to non-treated at t0 (before the addition of Triptolide). Results are the mean +/- standard deviation (SD) of one experiment, performed

with three biological replicates. No statistical analysis was performed, as only one experiment was performed.

Figure 6. Combinations of Pam3CSK4 with approved, clinically trialed and investigational drugs. Seven days post-infection, dHepaRG cells were treated twice either with drugs (Pam3CSK4 (P; 25ng/mL), IFN-α (I; 50IU/ml), TFV (T; 1 µM), JNJ-827 (C1, 1µM), JNJ-890 (C2; 1µM), FXR-α agonist (F; 100nM) and a kinase inhibitor, 1C8 (KINi; 5 µM)) in mono-, bi- or tri-therapies with the same concentrations, for a total exposure of treatment of 6 days. At the end of treatment, intracellular parameters (A) and secreted parameters (B) were quantified. Results are presented as % of NT conditions (one NT condition per plate was used). All histograms represent the mean of one experiment with three biological replicates and the error bars indicate SD.

Figure 1

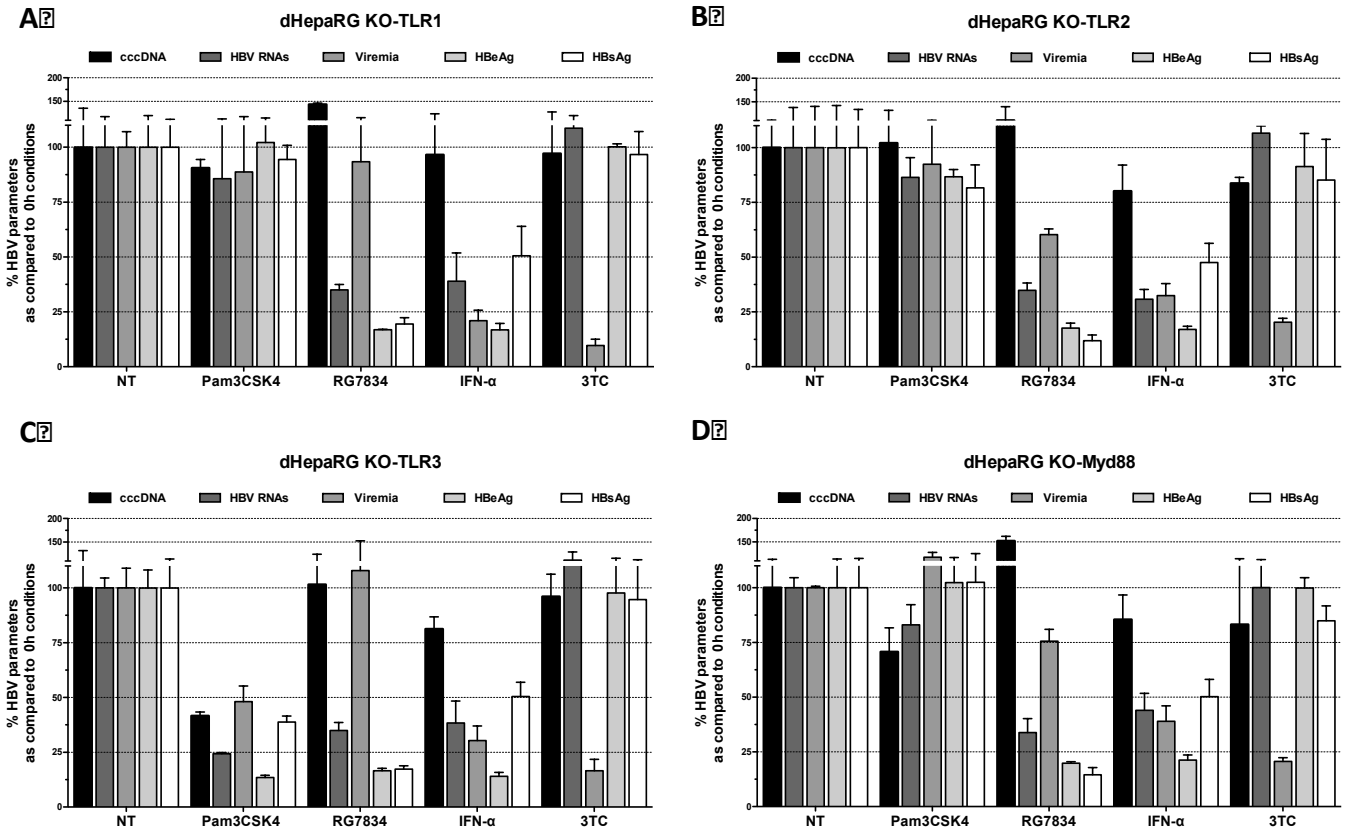
A
dHepaRG KO-TLR1
B
dHepaRG KO-TLR2
C
dHepaRG KO-TLR3
D
dHepaRG KO-Myd88
cccDNA
HBV RNAs
Viremia
HBeAg
HBsAg
% HBV parameters as compared to 0h conditions
NT
Pam3CSK4
RG7834
IFN-α
3TC

Figure 2

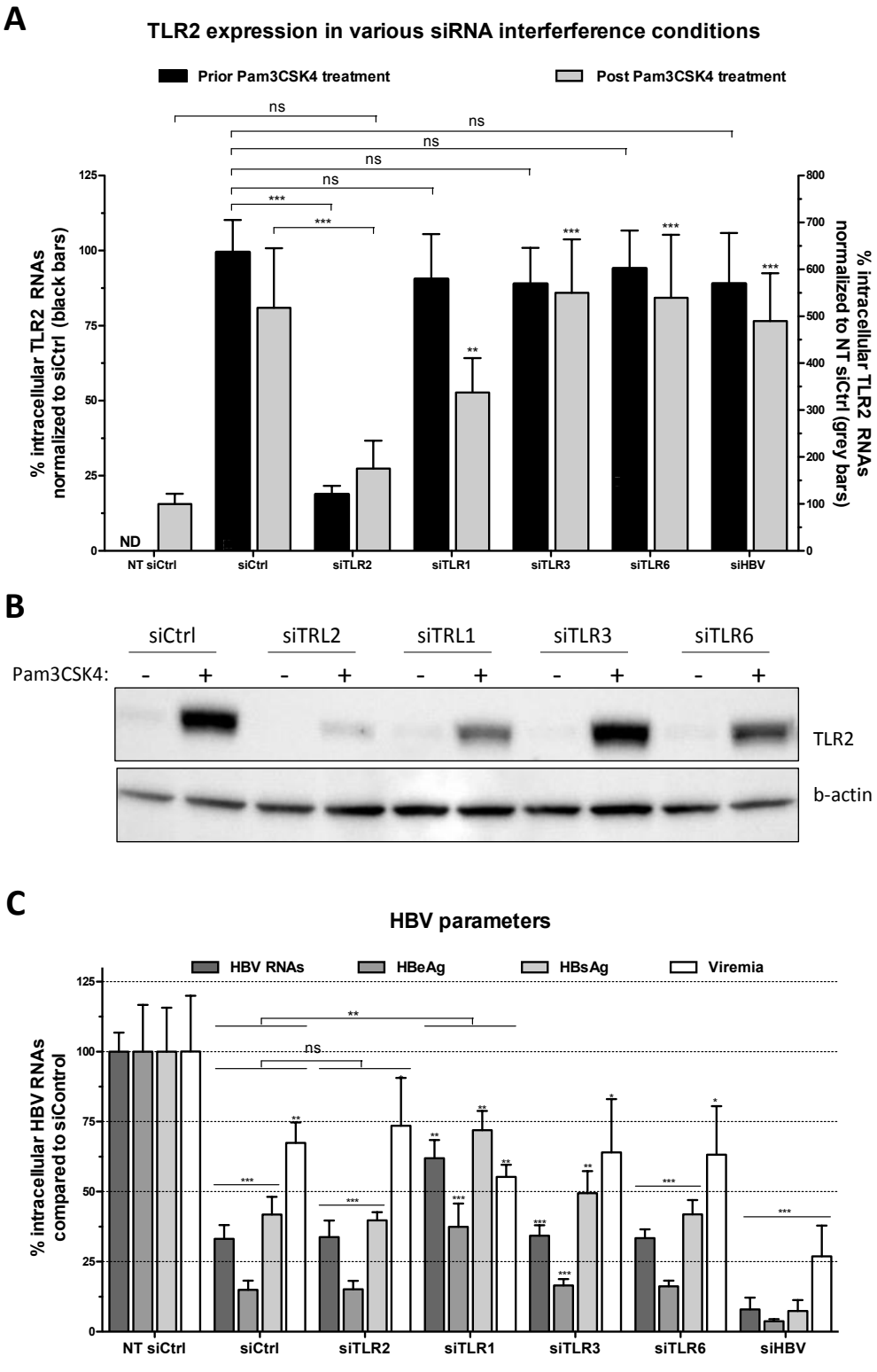
A
TLR2 expression in various siRNA interferference conditions
Prior Pam3CSK4 treatment
Post Pam3CSK4 treatment
% intracellular TLR2 RNAs normalized to siCtrl (black bars)
% intracellular TLR2 RNAs normalized to NT siCtrl (grey bars)
ND
NT siCtrl
siCtrl
siTLR2
siTLR1
siTLR3
siTLR6
siHBV
B
siCtrl
siTRL2
siTLR1
siTLR3
siTLR6
Pam3CSK4:
TLR2
b-actin
C
HBV parameters
HBV RNAs
HBeAg
HBsAg
Viremia
% intracellular HBV RNAs compared to siControl
NT siCtrl
siCtrl
siTLR2
siTLR1
siTLR3
siTLR6
siHBV

Figure 3

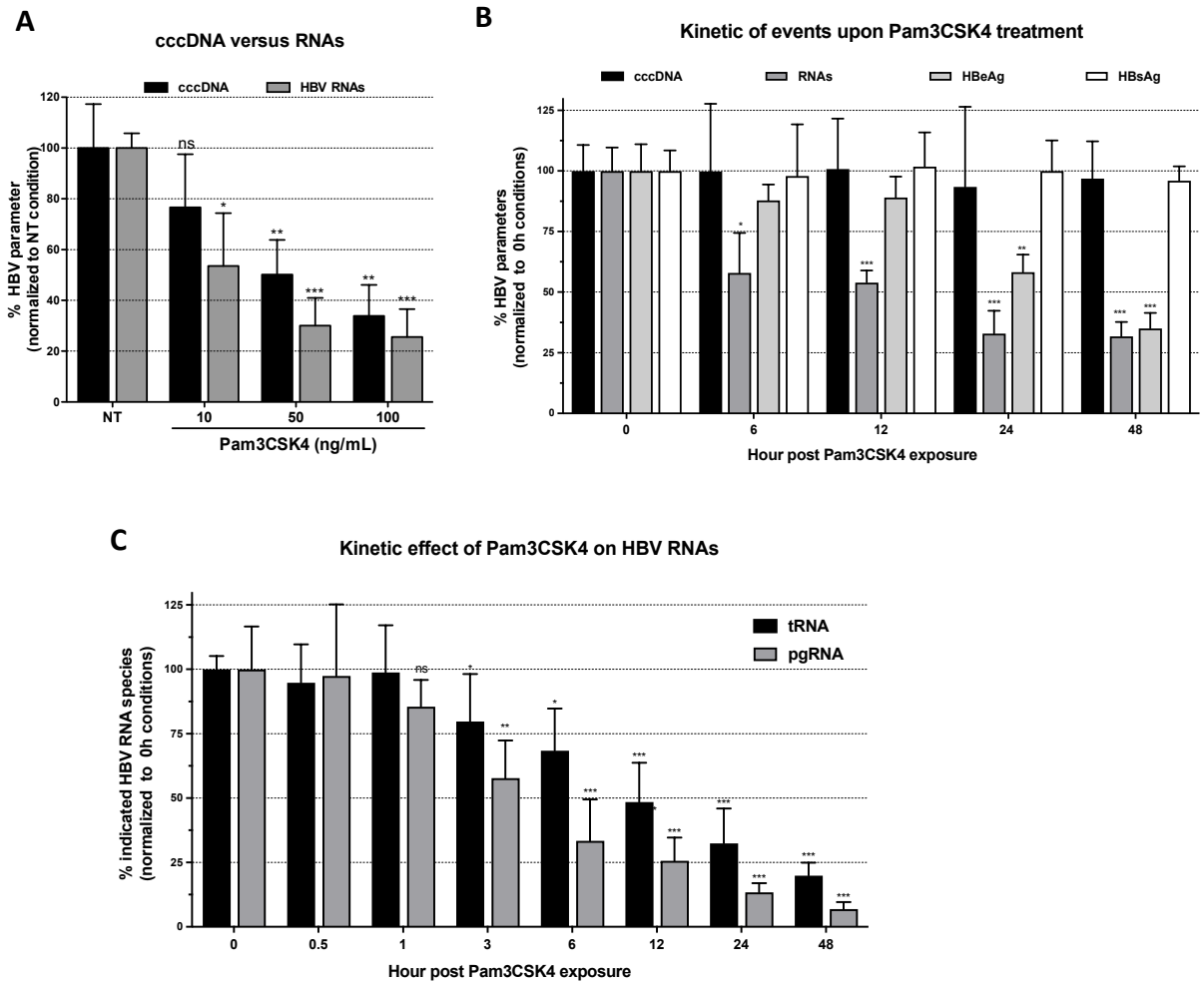
A
cccDNA versus RNAs
cccDNA
HBV RNAs
% HBV parameter (normalized to NT condition)
NT
10
50
100
Pam3CSK4 (ng/mL)
B
Kinetic of events upon Pam3CSK4 treatment
cccDNA
RNAs
HBeAg
HBsAg
% HBV parameters (normalized to 0h conditions)
Hour post Pam3CSK4 exposure
C
Kinetic effect of Pam3CSK4 on HBV RNAs
tRNA
pgRNA
% indicated HBV RNA species (normalized to 0h conditions)
Hour post Pam3CSK4 exposure

Figure 4

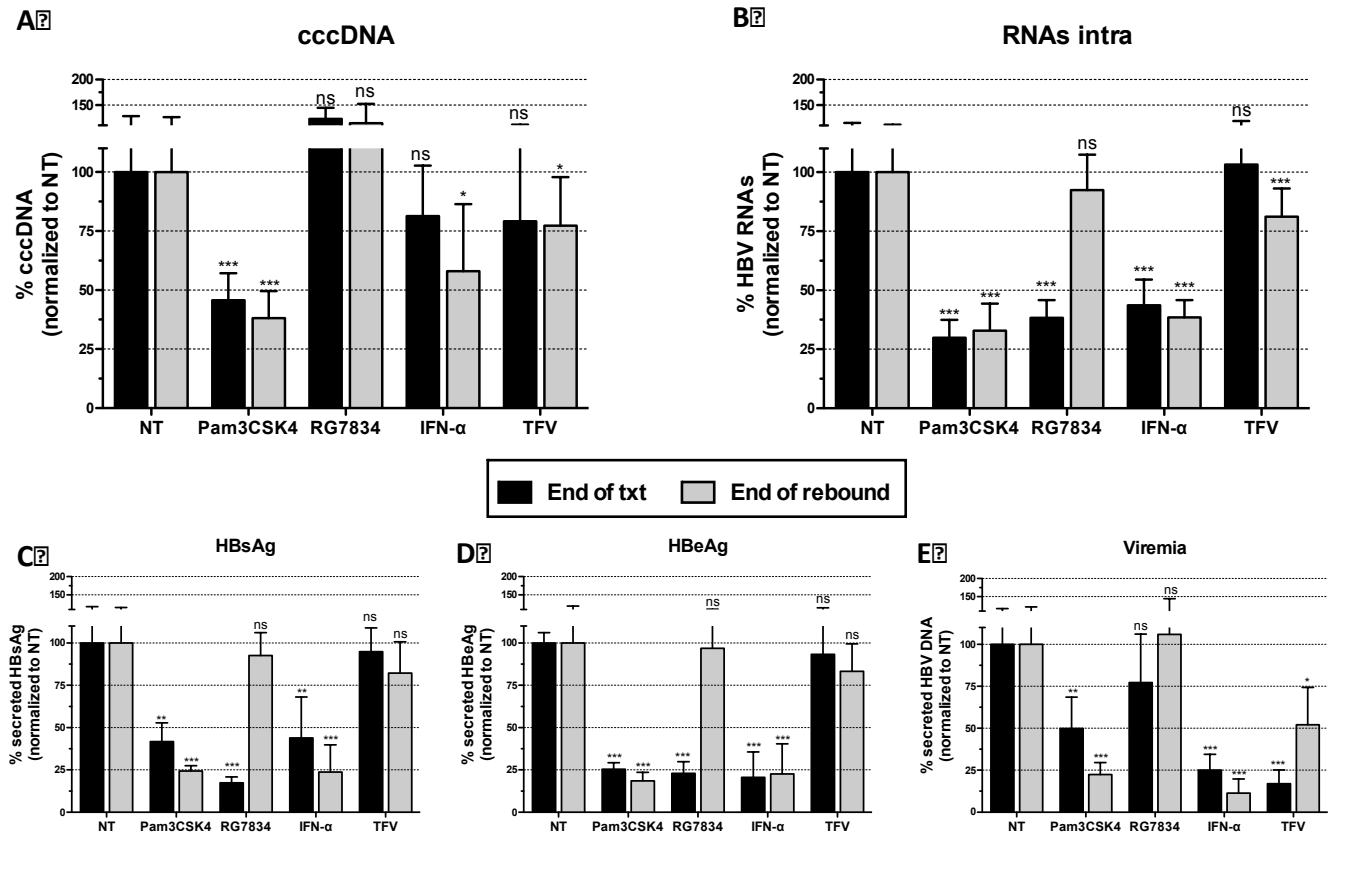

Figure 5

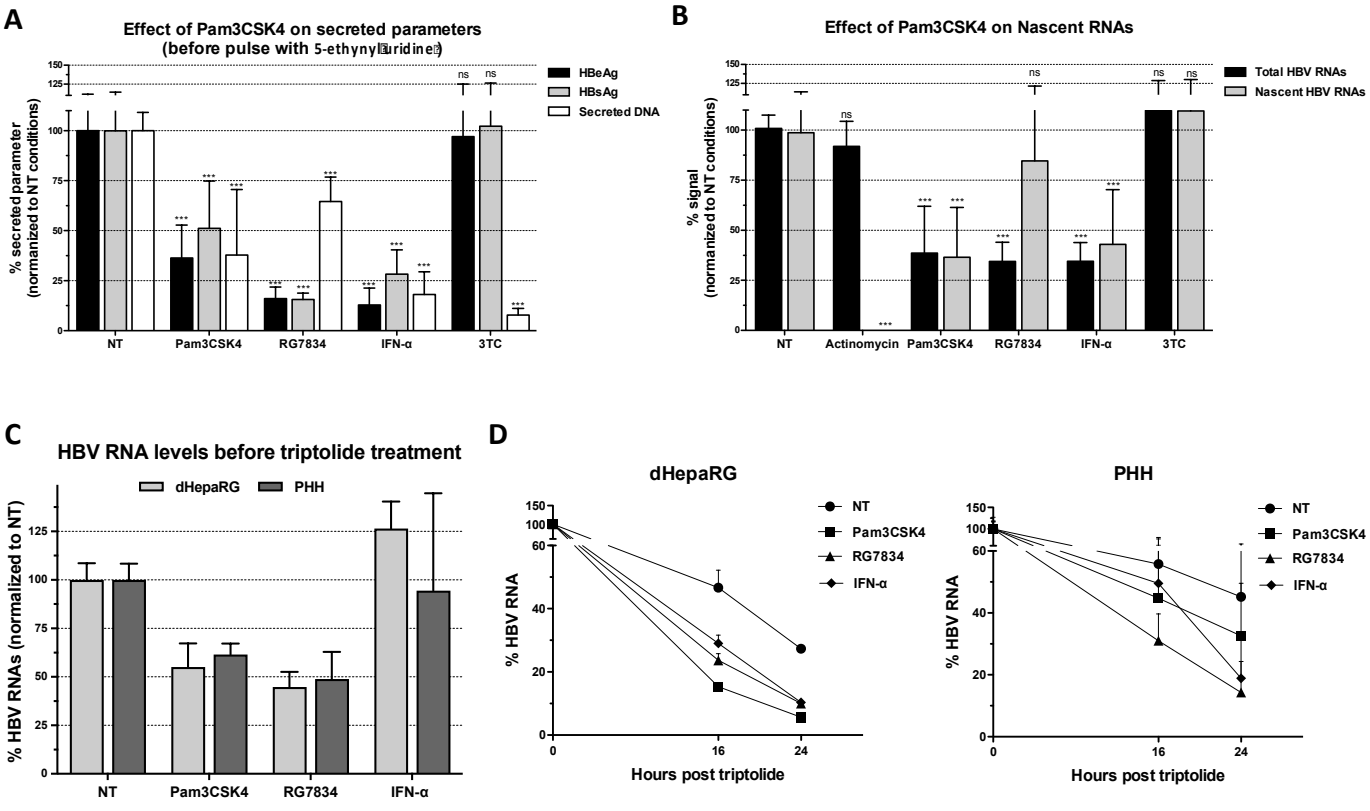

Figure 6

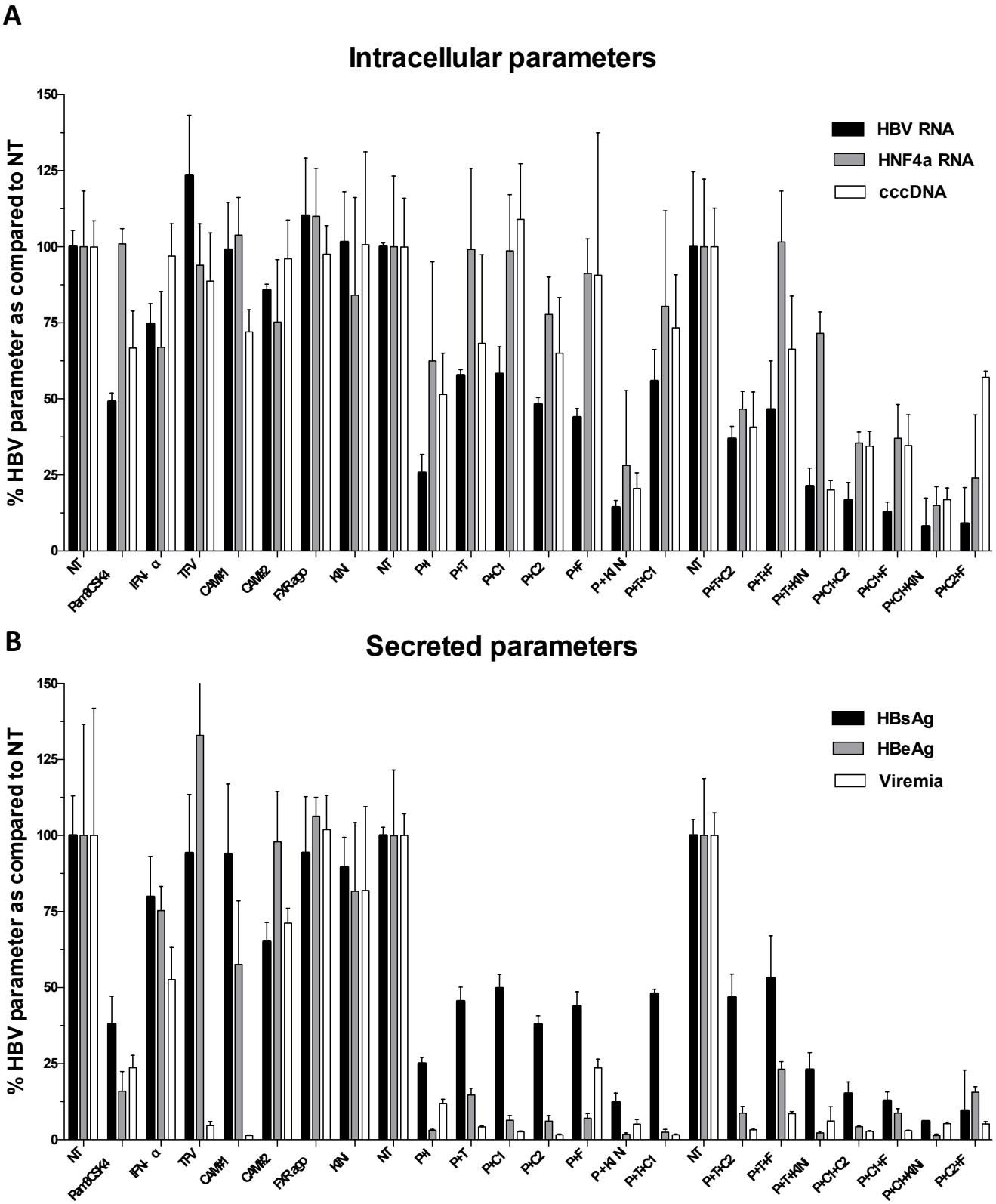
A
Intracellular parameters
% HBV parameter as compared to NT
HBV RNA
HNF4a RNA
cccDNA
B
Secreted parameters
% HBV parameter as compared to NT
HBsAg
HBeAg
Viremia
NT
ParmBCS4
IFN- α
TFV
CAMH1
CAMH2
FXRago
KIN
NT
PHJ
P+T
P+C1
P+C2
P+F
P+KIN
P+T+C1
NT
P+T+C2
P+T+F
P+T+KIN
P+C1+C2
P+C1+F
P+C1+KIN
P+C2+F

Supplementary Material and Methods

Table 1: Molecules used for treatments.

	References	Purchaser
Pam3CSK4	tlr-pms	InvivoGen
IFN-α	Prescription medicine	
RG7834	HY-117650A	Roche
Lamivudine	Prescription medicine	
GW4064	G5172	Sigma-Aldrich
LPS	00-4976-93	Invitrogen™
Actinomycin D	A9415	Sigma-Aldrich
Triptolide	T3652	Sigma-Aldrich
Cycloheximide	01810	Sigma-Aldrich

Table 2: Primers and probes sequences used in the studies.

		Sequences 5'->3' or References	Supplier
HBV (RNA)	Primer forward	ACCGAATGTTGCCCAAGGTC	Eurogentec
	Primer reverse	TATGCCTCAAGGTCGGTCGT	Eurogentec
PRNP	Primer forward	ACCGAGGCAGAGCAGT	Eurogentec
	Primer reverse	CCCCAGTGTTCCATCCTCC	Eurogentec
RPLP0	Primer forward	CACCATTGAAATCCTGAGTGATGT	Eurogentec
	Primer reverse	TGACCAGCCCAAAGGAGAAG	Eurogentec
HBA (Viremia)	Primer forward	GGAGGATACATAGAGGTTCCTTGA	Eurogentec
	Primer reverse	GTTGCCCGTTTGTCCTCTAATTC	Eurogentec
cccDNA	Primer forward	CCGTGTGCACTTCGCTTCA	Eurogentec
	Primer reverse	GCACAGCTTGGAGGCTTGA	Eurogentec
	Probe	[6FAM]CATGGAGACCACCGTGAACGCCC[BHQ1]	TIB MOLBIOL
Human β-globin		Hs00758889_s1	Life Technologies
GUSB		Hs99999908_m1	Life Technologies
pgRNA	Primer forward	GGAGTGTGGATTCGCACTCCT	Eurogentec
	Primer reverse	AGATTGAGATCTTCTGCGAC	Eurogentec
	Probe	[6FAM]AGGCAGGTCCCCTAGAAGAAGAACTCC[BHQ1]	TIB MOLBIOL
TLR1	Primer forward	ACAAGCAGGTTGTCTTGTGTT	Eurogentec
	Primer reverse	GAGGGCCTGGTACCCCTATT	Eurogentec
TLR2	Primer forward	CTCTGGTGCTGACATCCAATGGAA	Eurogentec
	Primer reverse	GGGCTTGAACCAGGAAGACGATAA	Eurogentec
TLR3	Primer forward	AGAAGGTTTTCGGGCCAGCTTT	Eurogentec
	Primer reverse	TGACAGCTCAGGGATGTTGGTATG	Eurogentec
TLR6	Primer forward	ACCCATTCCACAGAACAGCATTCC	Eurogentec
	Primer reverse	TCCTTGGGCCACTGCAAATAAGTC	Eurogentec
Fen1	Primer forward	GCCAATCCAGGAATTCCACC	Eurogentec
	Primer reverse	GATTCGCTCCTCAGAGAACTGCTT	Eurogentec
MCPIP1	Primer forward	AACTGGAGAAGAAGAAGATCCTGG	Eurogentec
	Primer reverse	ATTGACGAAGGAGTACATGAGCAG	Eurogentec
HNF4α	Primer forward	GAGTGGGCCAAGTACA	Eurogentec
	Primer reverse	GGCTTTGAGGTAGGCATA	Eurogentec
APOBEC3B	Primer forward	GACCCTTTGGTCCTTCGAC	Eurogentec
	Primer reverse	GCACAGCCCCAGGAGAAG	Eurogentec

Table 3: Purchaser and reference list of different antibodies used in the studies

Target	Purchasers	References
FEN1	Abcam	Ab17994
TLR1	Cell Signalling	2209S
TLR2	Cell Signalling	12276S
TLR3	Cell Signalling	6961S
TLR6	Cell Signalling	12717S
MCPIP1	GeneTex	GTX110807
NF-κB p65	Cell Signalling	8242S
Phospho-NF-κB p65	Cell Signalling	3033S
NF-κB2 p100/p52 (WB)	Cell Signalling	4882S
NF-κB2 p100/p52 (IP)	Cell Signalling	37359S
RelB	Cell Signalling	10544S
NF-κB p105/p50	Cell Signalling	3035S
Actin-β	Sigma	A2228
Goat Anti-Mouse Immunoglobulins/HRP	Dako	PO447
Goat Anti-Rabbit Immunoglobulins/HRP	Dako	PO448
HBc	ThermoFisher	MA1-7609
H3K27Ac	Diagenode	C15410196
NF-κB p65	Millipore	17-10060
HBsAg	Abbott	MAb H166
HBsAg (F35.25)	-	-
HNF4α	Abcam	ab41898

Table 4: Sequences of siRNAs with references and purchaser used in studies.

	Target sequences	References	Purchaser
siControl	GCCCUUCUCUGCAGUCAAG	D-001810-01-50	Dharmacon
siHBV	CGACCUUGAGGUAUACUUCUU	Custom	Dharmacon
siFEN1	GGUGAAGGCUGGCAAAGUC GGGUCAAGAGGCUGAGUAA CAAACUAAUUGCUGAUGUG CAAGUACCCUGUGCCAGAA	L-010344-00-0005	Dharmacon
siTLR1	GGCAAUAUGUCUCAACUAA CCGCAGUACUCCAUUCCUA CCAAUUGCUCAUUUGAAUA GUUGAGCACCACACACUUA	L-008086-00-0005	Dharmacon
siTLR2	AAAUCUGAGAGCUGCGAUA AGGUAAAGUGGAAACGUUA UGUUUGGAACUGCGAGAUA AGUAGGAAUGCAAUAACUA	L-005120-01-0005	Dharmacon
siTLR3	GAACUAAAGAUCAUCGAUU CAGCAUCUGUCUUUAAUAA AGACCAAUCUCUCAAAUUU UCACGCAAUUGGAAGAUUA	L-007745-00-0005	Dharmacon
siTLR6	GGUGAAAAGUGAAUUGGUA CAACUAGUUUAUUCGCUAU GCACCAAGCACAUUCAAGU CCUGUGGAAUAUCUCAAUA	L-005156-00-0005	Dharmacon
siAPOBEC3B	CACAUGGGCUUUCUAUGCA CCUGAUGGAUCCAGACACA UGACCUACGAUGAGUUUGA GUGAUUAAUUGGUCCAUA	L-017322-00-0005	Dharmacon

Table 6: sgRNA designed for lentiCRIPR and generation of dHepaRG-Cas 9 KO cell lines.

	Position	Strand	Sequences	PAM	Exon	Specificity Score	Efficiency Score
TLR1	58784	-1	CACCGTTGTATGCCAAACCAGCTGG AAACCCAGCTGGTTTGGCATACAAC	AGG	4	41.1574669	69.5526439540046
	58510	1	CACCGGGTCTTAGGAGAGACTTATG AAACCATAAGTCTCTCCTAAGACCC	GGG	4	41.6546525	65.3708047572652
TLR2	153703850	1	CACCGTGGAAACGTTAACAATCCGG AAACCCGGATTGTTAACGTTTCCAC	AGG	1	93.1811822	74.87917659622852
	153703124	1	CACCGTTAGCAACAGTGACCTACAG AAACCTGTAGGTCACTGTTGCTAAC	AGG	1	68.0714882	73.43170064056989
TLR3	12409	-1	CACCGGGAAATTAACGGGACCACCG AAACCGGTGGTCCCGTTAATTTCCC	GGG	6	48.0648961	75.48276420451064
	11614	-1	CACCGAACCGTTGCCGACATCATGG AAACCCATGATGTCGGCAACGGTTC	AGG	6	46.4477338	71.11165548506018
MyD88	38138900	1	CACCGCCGGCAACTGGAGACACAAG AAACCTTGTGTCTCCAGTTGCCGGC	CGG	1	60.374396	68.93936884860913
	38138815	1	CACCGTGTCTCTGTTCTTGAACGTG AAACCACGTTCAAGAACAGAGACAC	CGG	1	75.6193589	65.1594894182281

Figure Sup 1

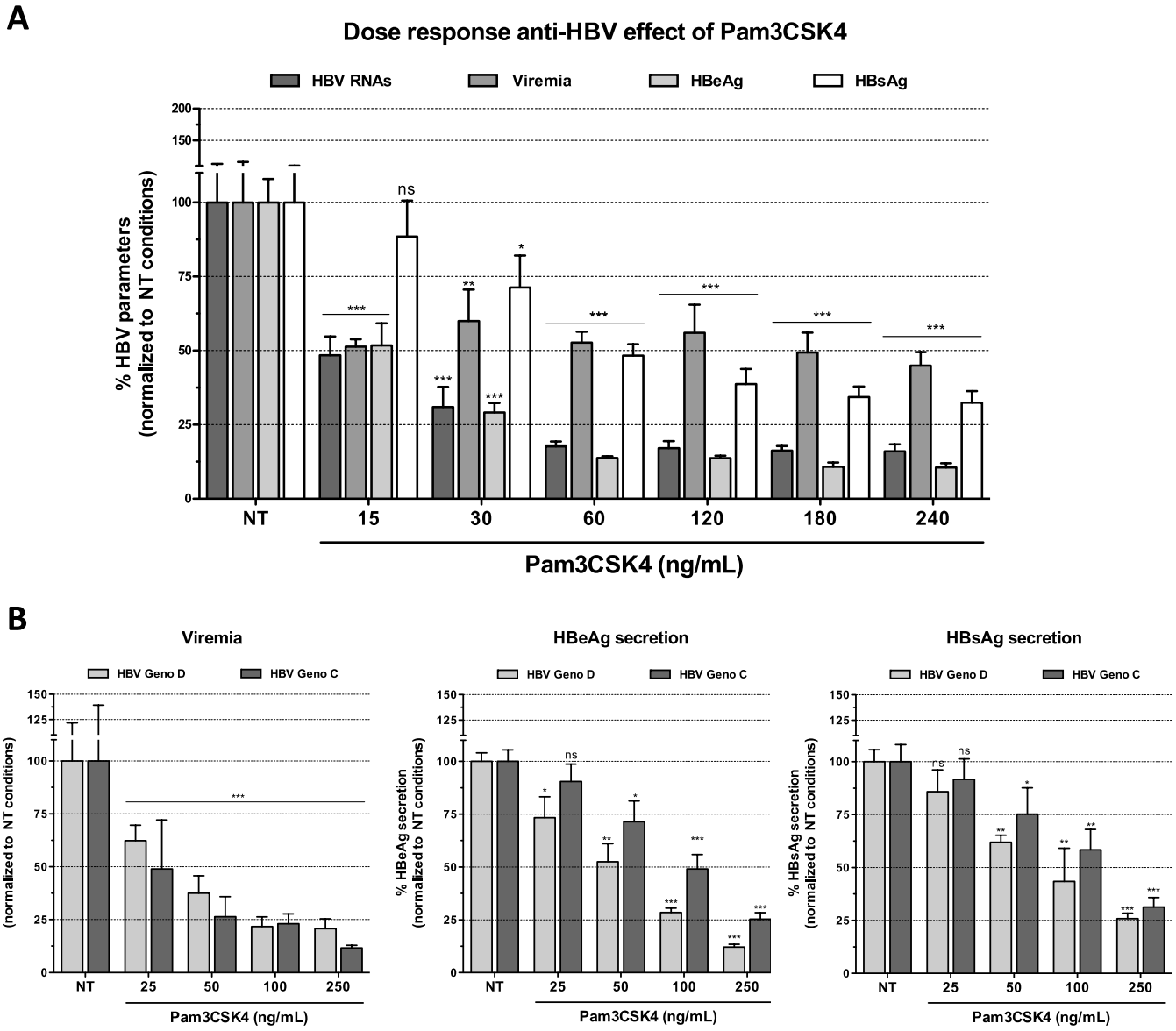

Figure Sup 1. Pam3CSK4 has broad and potent anti-HBV activity in HBV infected hepatocytes. Differentiated HepaRG were infected with 100vge/cell of HBV genotype D or C. At day-7 post-infection, cells were either non-treated (NT; saline control) or treated twice every three-other-days with indicated concentrations of Pam3CSK4. At day-13 post-infection (i.e. day 6 post-treatment), cells and supernatants were harvested for analyses. The effect on HBV RNAs, secreted HBV antigens, and viremia were respectivelly quantified by RT-qPCR, CLIA, and qPCR. Results are the mean +/- standard deviation (SD) of 2 independent experiments, each performed with three biological replicate and statistical analyses were performed using Mann-Whitney tests. Statistically significant differences from NT conditions are indicated by asterisks (ns: non-significant, *P<0.05, **P<0.005, ***P<0.0001).

Panel A: Dose response of Pam3SCK4 on various HBV parameters. Results are presented in percentage (%) and are normalized to NT conditions.

Panel B: Effect of Pam3SCK4 on two HBV genotypes.

Figure Sup 2

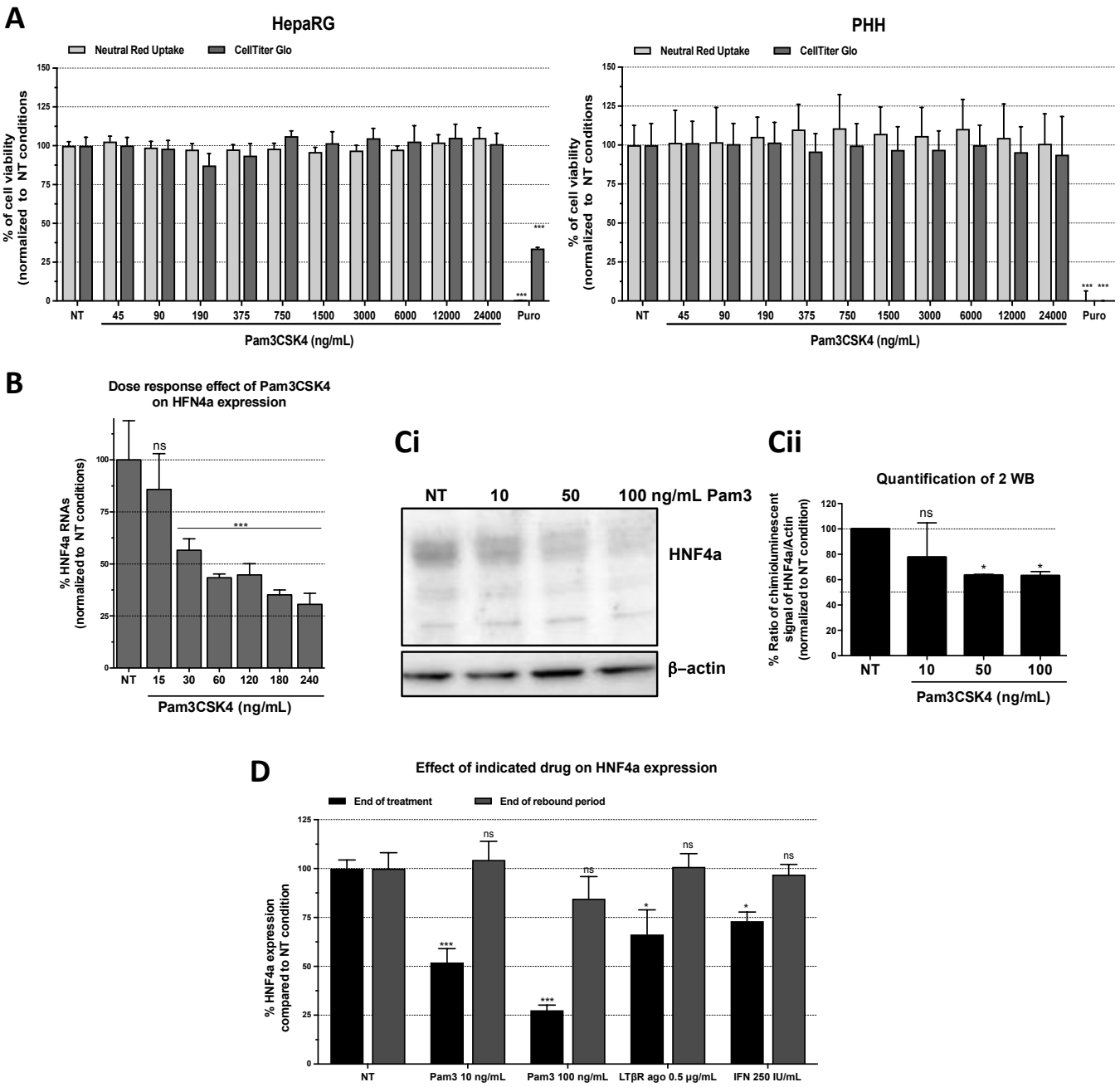

Figure Sup 2. Pam3CSK4 is not cytotoxic in hepatocytes, but induces a reversible loss of HNF4a expression. **A)** Differentiated HepaRG cells and PHH were treated twice every three-other-day with indicated concentrations of Pam3CSK4 (in ng/mL) for a total exposure time of 6 days. Neutral red uptake and Cell-Titer-Glo luminescent cell viability assays were then performed. All histograms represents 16 biological replicates (done in two batches of cells), expressed in percentage and normalized to non-treated condition (NT) and the error bars indicate SD.
B) RNA expression of HNF4a was analysed by RTqPCR on total RNA extracted from HepaRG cells treated twice every three-other-day with indicated concentrations of Pam3CSK4 (in ng/mL). **C)** Similar to B, HNF4a protein expression analysed by western blot and its densitometric quantification. **D)** Differentiated HepaRG cells were treated twice every three-other-day with indicated drugs and concentrations for a total exposure time of 6 days, than left without treatlent for additional 14 days. RNA were extracted at the end of the treatment and end of the rebound period and RTqPCR was done on HNF4a.
Statistically significant differences from NT conditions are indicated by asterisks (ns: non-significant, *P<0.05, **P<0.005, ***P<0.0001).

Figure Sup 3

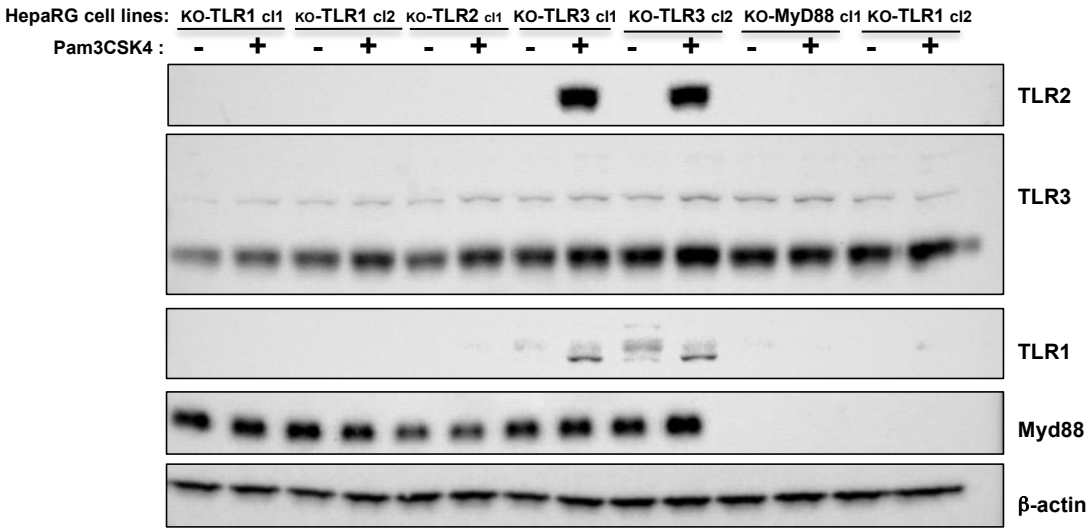

Figure Sup 3. Checking of the invalidation of genes in KO HepaRG cell lines. Protein extracts (in RIPA buffer) coming from indicated cell lines (2 clones/cell line except for HepaRG-KO-TLR2) which have been stimulated or not with Pam3CSK4 at 100 ng/mL for 24h were subjected to western blot analyses with indicated antibodies.

Figure Sup 4

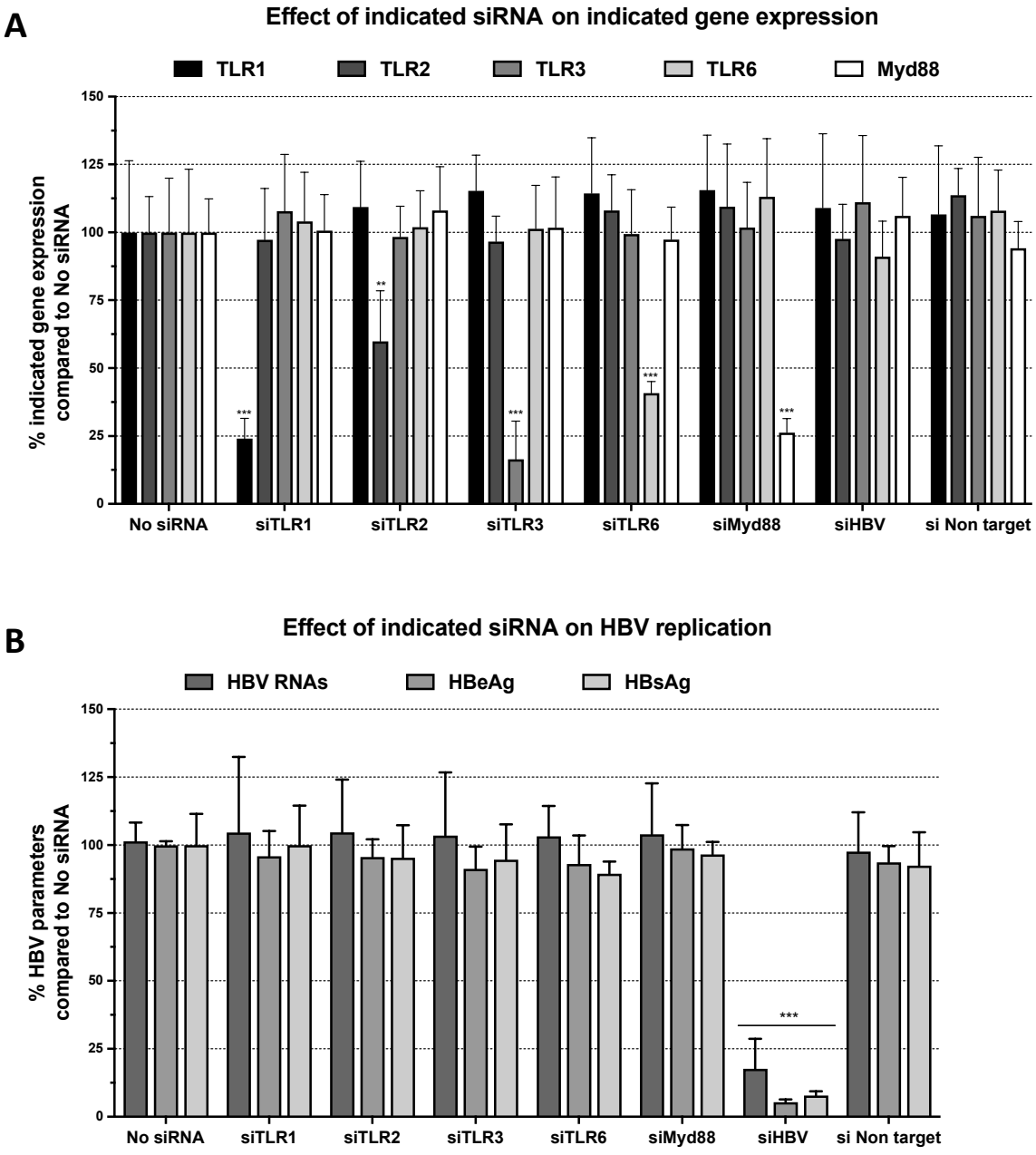

Figure Sup 4. Effect of the invalidation of TLR1, TLR2, TLR6 and Myd88 (and controls) on the basal replication of HBV. Differentiated HepaRG cells were infected with HBV with 100 vge/cell and 7 days post infection, cells were transfected once with siRNAs targeting either TLR1, TLR2, TLR6 or Myd88, as well as controls siRNAs (targeting TLR3 or HBV or an irrelevant target). Six days post-transfection, supernatants were collected for quantification by CLIA of HBeAg and HBsAg and RNAs were extracted from cells for RTqPCR analyses. **A)** Effect of indicated siRNAs, or controls, on the expression of indicated genes. **B)** Effect of indicated siRNAs, or controls, on HBV parameters. Results are presented in %, normalized to the no siRNA conditions. Results are the mean +/- standard deviation (SD) of 3 independent experiments (n=3), performed with three biological replicates. Statistically significant differences from No siRNA conditions are indicated by asterisks (ns: non-significant, *P<0.05, **P<0.005, ***P<0.001).

Figure Sup 5

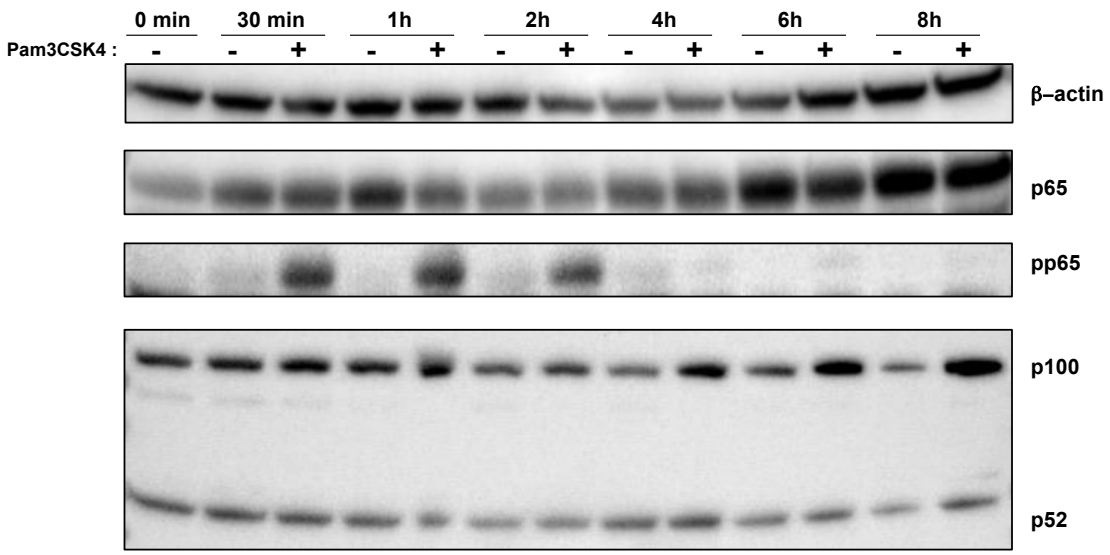

Figure Sup 5. Kinetic of activation of the NF-κB canonical pathway by Pam3CSK4. dHepaRG were treated 7 days post-infection with Pam3CSK4 (100 ng/mL). Protein lysates were generated at different time points to analyse by western blotting the levels of p65, phosphorylated p65 (pp65), p100, and p52 in link with activation of both canonical and non-canonical of NF-κB pathways.

Figure Sup 6

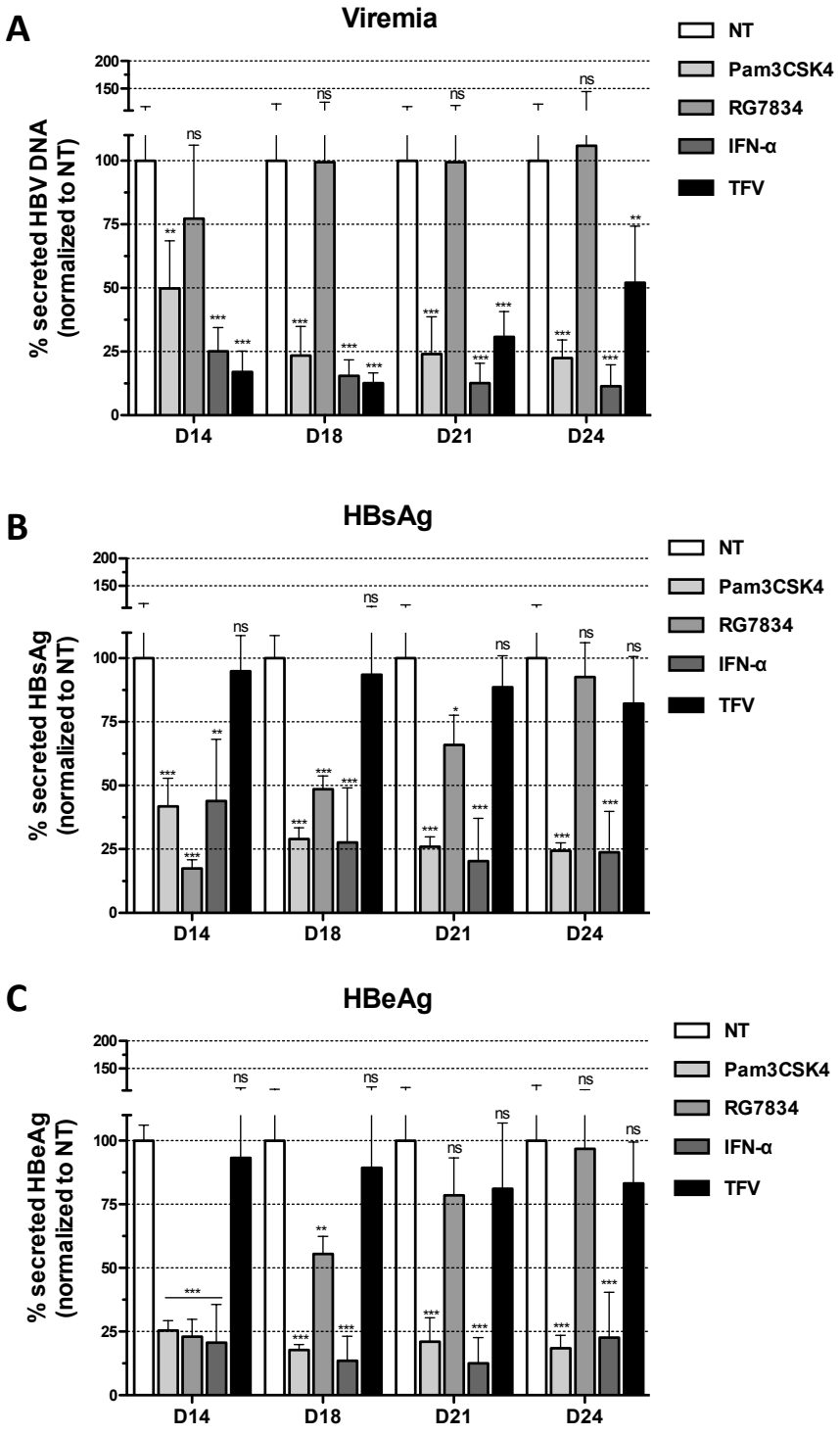

Figure Sup 6. Pam3CSK4 induces a long-lasting antiviral effect. Seven days post-infection, dHepaRG were treated twice with Pam3CSK4 (100ng/mL), IFNα (500 IU/mL), RG7834 (0.1µM), Tenofovir (TFV ; 1µM) for a total exposure time of six days. Secreted HBV parameters were analyzed 14 days post-infection (at the end of treatment), and 24 days post-infection, as well as in-between (D18 and D21) in kinetic. The effect on viremia **(A)** and secreted HBV antigens **(B and C)**, were respectively quantified by qPCR and CLIA. All histograms represent the mean of at least three independent experiments with three biological replicates and the error bars indicate SD. Statistically significant differences from NT conditions are indicated by asterisks (ns: non-significant, *P<0.05, **P<0.005, ***P<0.001).

Figure Sup 7

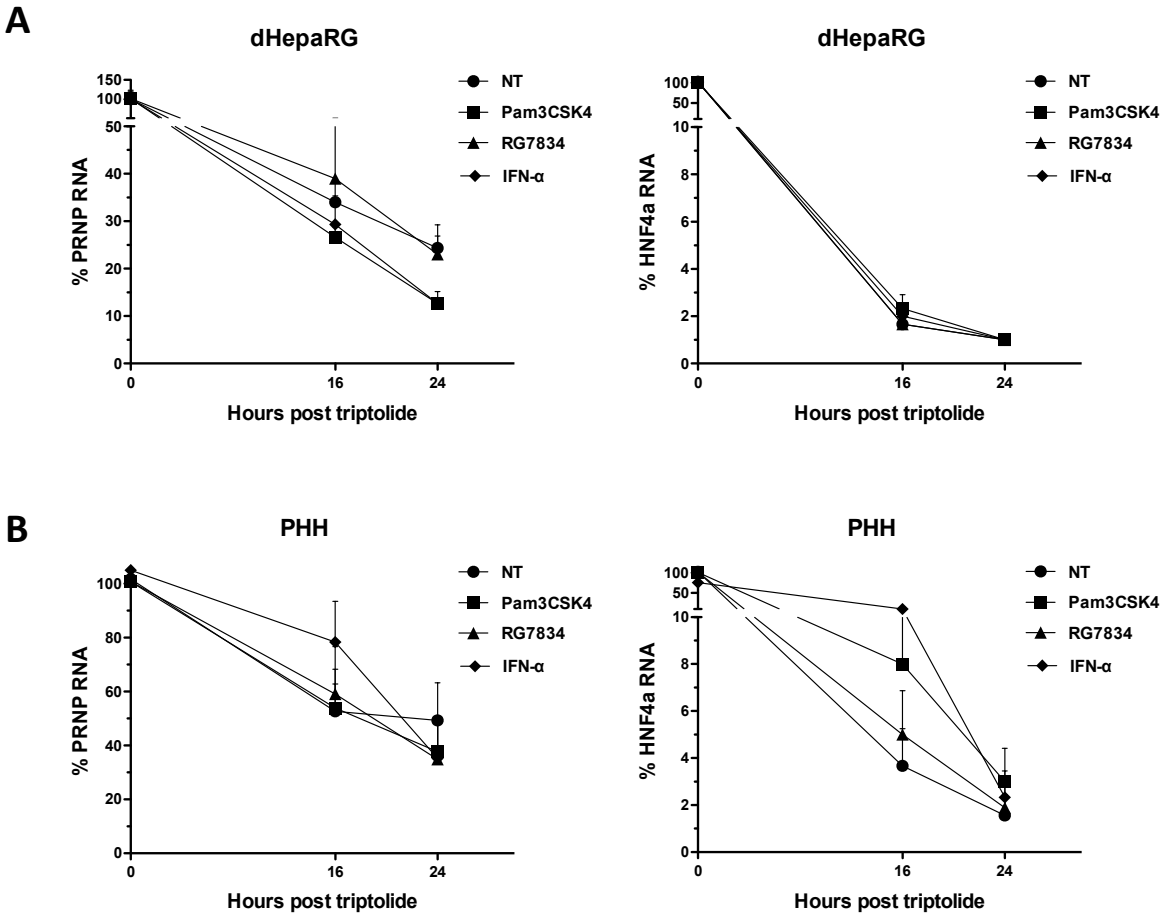

Figure Sup 7. Controls for RNA decay analyses. Infected dHepaRG **(A)** or PHH **(B)** were treated with Pam3CSK4 (1µg/mL for PHH and 100ng/mL for dHepaRG), RG7834 (0.1 µM) and Peg-IFN-α (1000 IU/mL) for three days prior to the addition of triptolide (1µg/mL). Triptolide was added to cell medium (yet containing treatment). At indicated time RNAs were extracted and quantified by RTqPCR with HBV primers and house-keeping genes (PRNP and HNF4α) ; normalization was done to non-treated at t0 (before the addition of Triptolide). Results are the mean +/- standard deviation (SD) of one experiment, performed with three biological replicates. No statistical analysis was performed, as only one experiment was performed.

Figure Sup 8

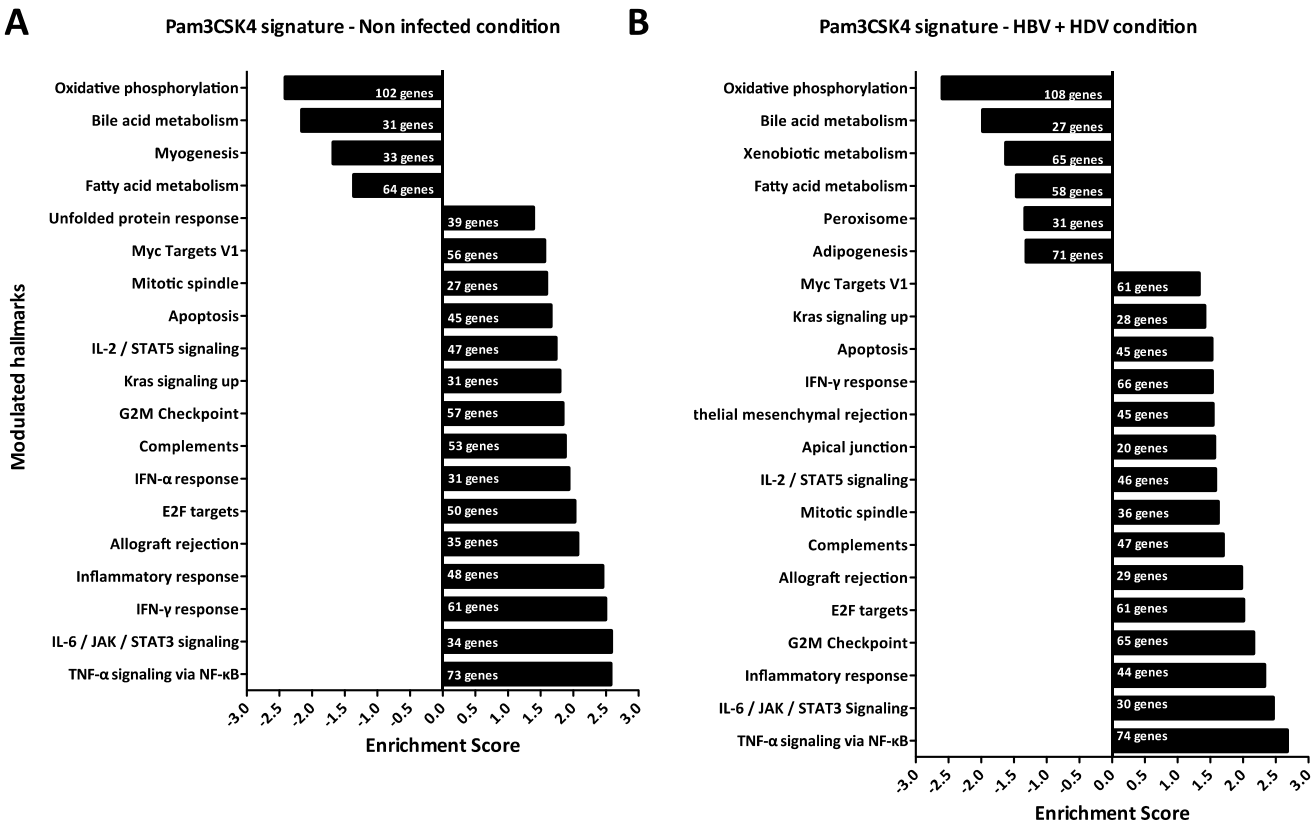

Figure Sup 8. Biological pathways regulated by Pam3CSK4 in both non-infected and infected conditions. A) and **B)** dHepaRG cells were co-infected with HBV (100 vge/cell) and HDV (10 vge/cell). Cells were treated 6 days after infection with Pam3CSK4 (100 ng/mL). 48 hours post treatment HBV RNAs were analysed, quantified to ensure antiviral activity of Pam3CSK4 by RT-qPCR, and they were then sequenced. Fold change of genes were calculated in a differential manner comparing modulation of genes in infected conditions with modulation of genes in non-treated conditions, getting rid of genes modulated by the viruses. Up-regulated or down-regulated genes with a p-value-adj< 0.05 have been selected for further analysis. List of genes have been submitted to GSEA software (using MSigDB) to identify modulated pathways. Results are the mean of an experiment with two biological replicates and are represented in bar-plots (FDR<0.25).

Figure Sup 9

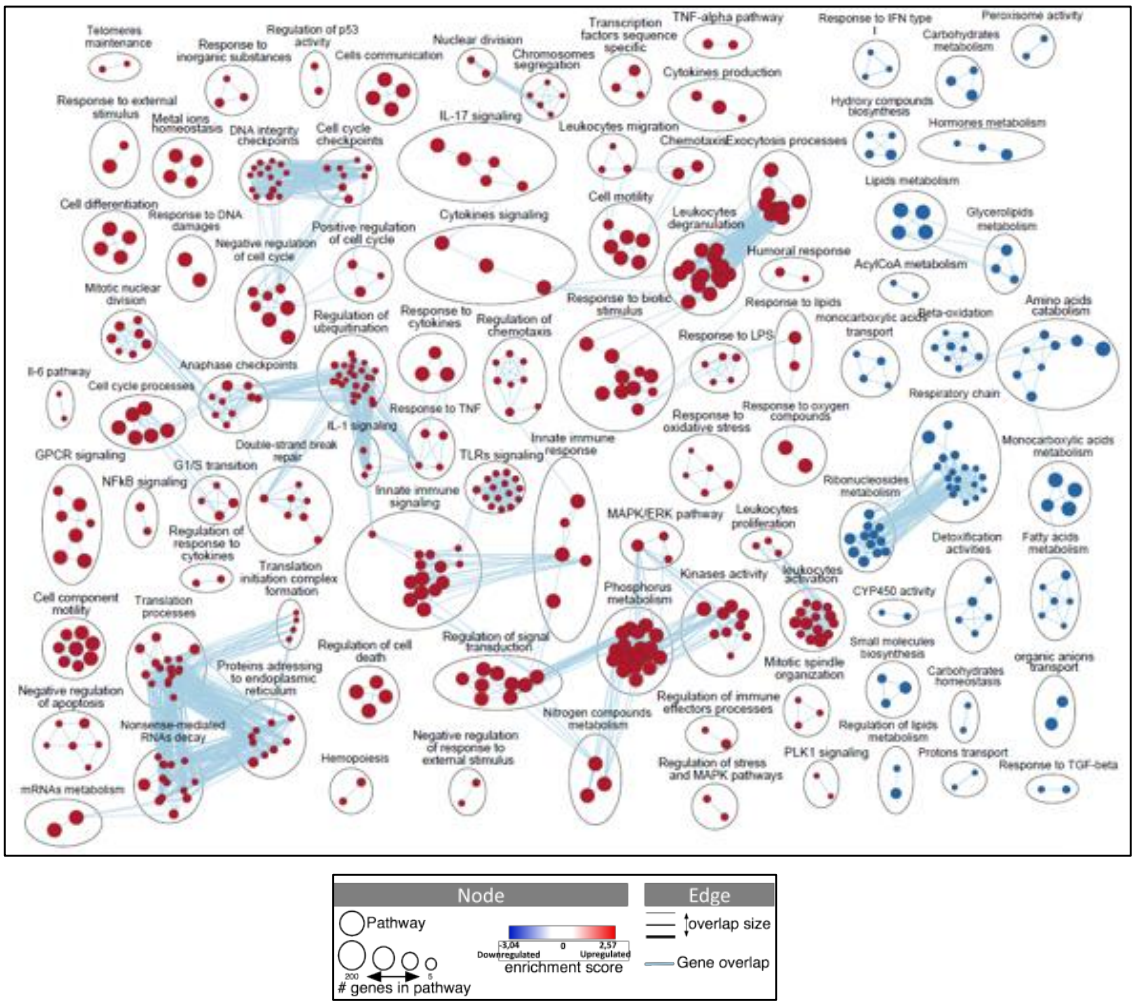

Figure Sup 9. Biological pathways regulated by Pam3CSK4. Differentiated HepaRG cells were co-infected with HBV (100 vge/cell) and HDV (10 vge/cell). Cells were treated 6 days after infection with Pam3CSK4 (100 ng/mL). 48 hours post treatment HBV RNAs were analysed, quantified to ensure antiviral activity of Pam3CSK4 by RT-qPCR, and they were then sequenced. Fold change of genes were calculated in a differential manner comparing modulation of genes in infected conditions with modulation of genes in non-treated conditions, getting rid of genes modulated by the viruses. Up-regulated or down-regulated genes with a p-value-adj< 0.05 have been selected for further analysis. List of genes have been submitted to GSEA software (using MSigDB database) to identify modulated pathways. Modelling was realized using Cytoscape software and application Enrichment-Map (FDR<0.1; Node cut-off <0.1; Edge cut-off <0.3). Clusters have been generated by Auto-Annotate application.

Figure Sup 10

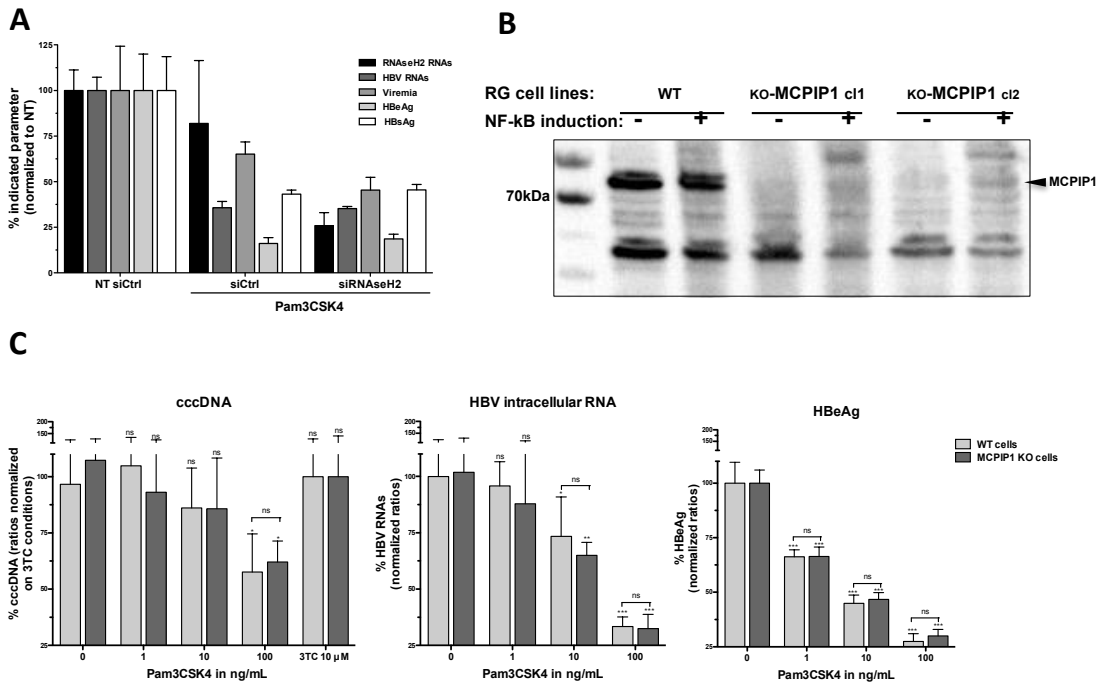

Figure Sup 10. RNAseH2 and MCPIP1 are not involved in Pam3CSK4-induced anti-HBV inhibitory phenotypes. Differentiated HepaRG were infected with HBV (100 vge/cell) and at least 7 days post infection, cells were transfected once with siRNAs directed to RNASEH2A. Four days post-transfection, cells were treated two times with Pam3CSK4 (100ng/mL) for a total exposure time of 6 days. **A)** HBV RNAs were quantified by RT-qPCR, expressed in percentage, normalized to housekeeping gene level and non-treated si-control condition (NT siCtrl); effects on HBV antigens were quantified by CLIA in supernatants, expressed in percentage and normalized to NT siCtrl; effects on viremia were quantified by qPCR, according to a standard curve (build with dilutions of a plasmid containing the HBV sequence. All histograms represent the mean of two independent experiments with three biological replicates and the error bars indicate SD. **B)** Expression of MCPIP1 in wild type and CRISPR-Cas9 enginered HepaRG cell lines. **C)** Differentiated HepaRG cells (wWT and MCPIP1-KO) were infected with HBV (100 vge/cell) and at least 7 days post infection, cells were treated two times with Pam3CSK4 (100ng/mL) for a total exposure time of 6 days. The effect on cccDNA, HBV RNAs, and secreted HBeAg antigen were respectively quantified by cccDNA-specific-qPCR, RT-qPCR, and CLIA. All histograms represent the mean of at least three independent experiments with three biological replicates and the error bars indicate SD. Statistically significant differences from NT conditions are indicated by asterisks (ns: non-significant, *P<0.05, **P<0.005, ***P<0.001).

Figure Sup 11

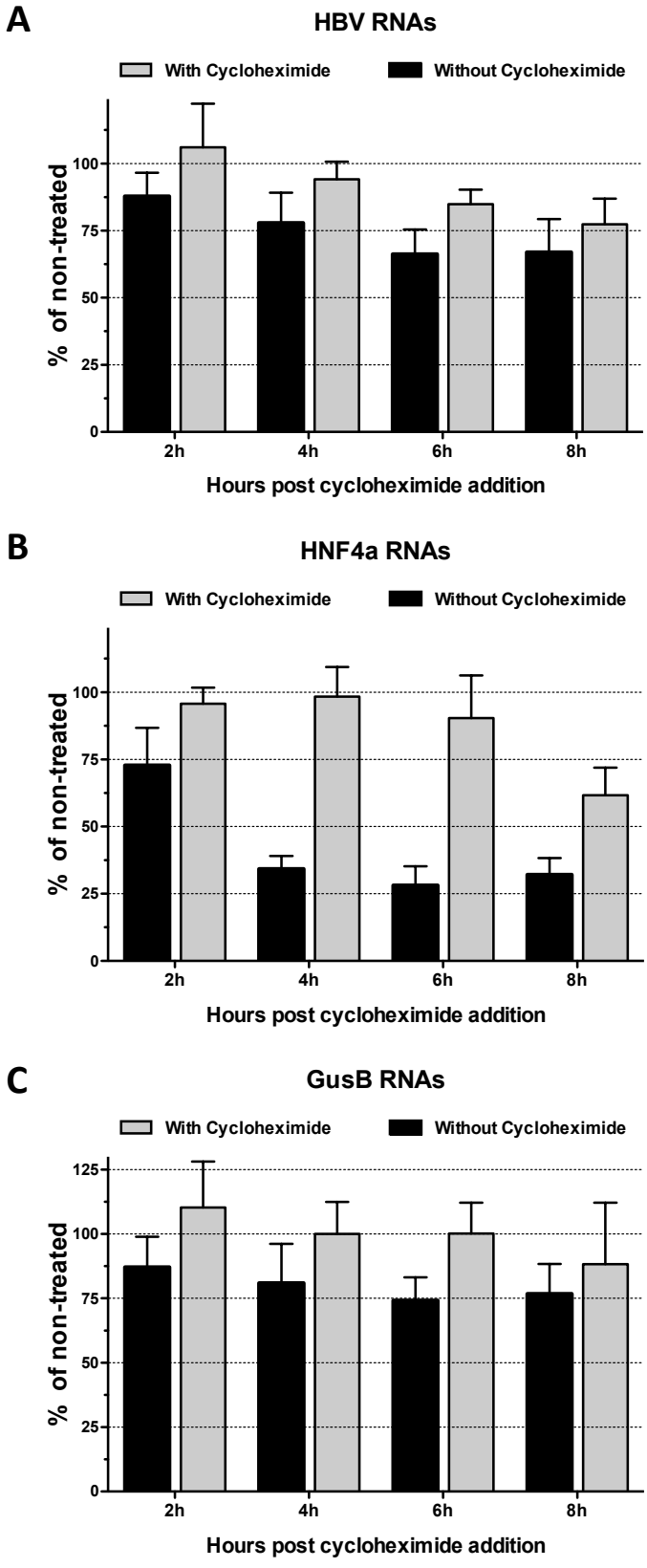

Figure Sup 11. Pam3CSK4 does not seem to induce the synthesis of new effector to degrade RNAs. Seven days post-infection, dHepaRG were treated with Pam3CSK4 (100ng/mL) with or without cycloheximide (100µg/mL). HBV **(A)**, HNF4α **(B)** and GusB **(C)** RNAs, were analysed at indicated time points, quantified and normalized to housekeeping gene PRNP and non-treated of indicated time point. All time points represent the mean of four independent experiments of three biological replicates and the error bars indicate SD.

Figure Sup 12

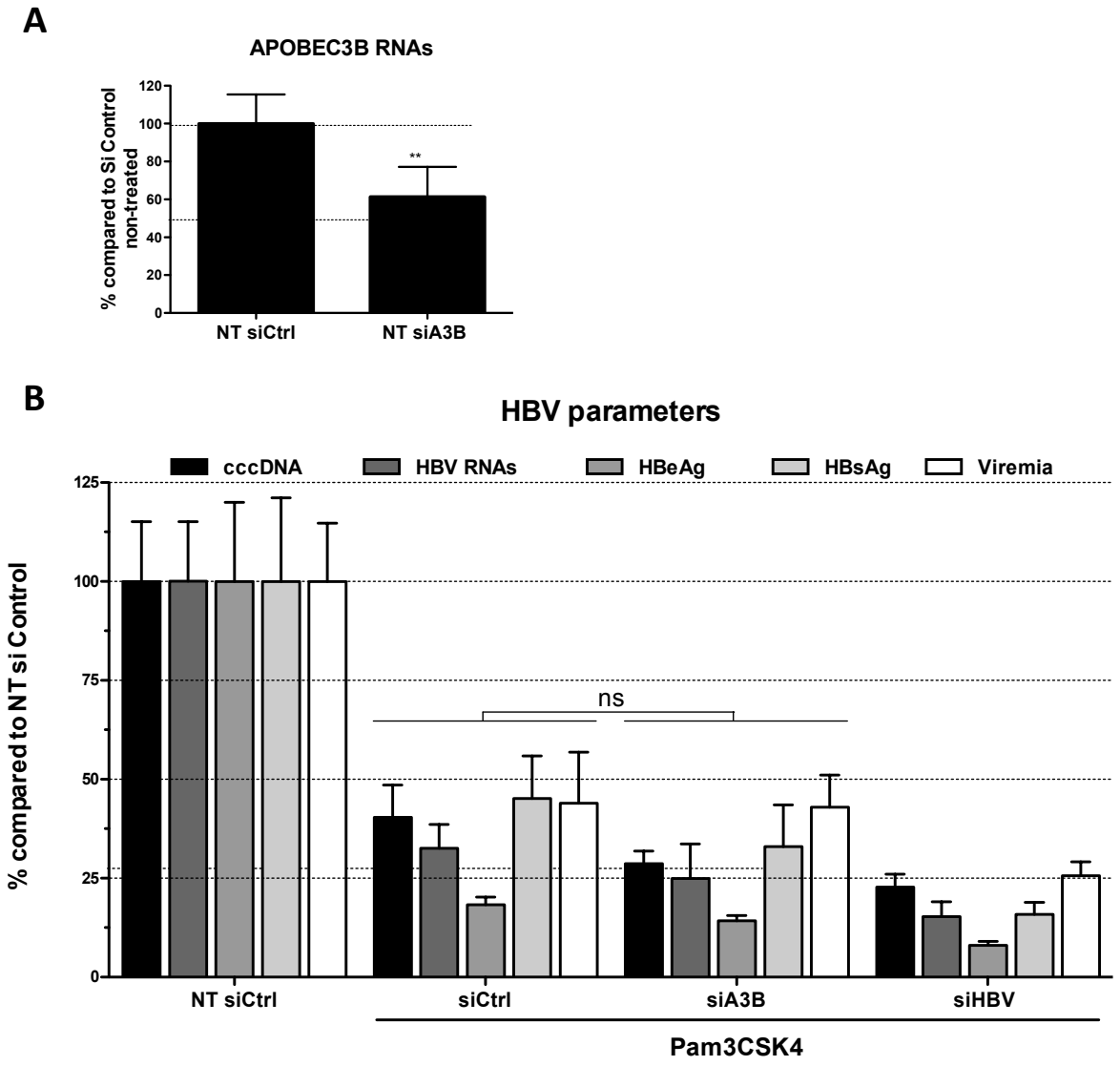

Figure Sup 12. Pam3CSK4-induced antiviral effect on cccDNA is not due to APOBEC3B. DHepaRG were infected and at least 7 days post infection, cells were transfected once with siRNAs directed to APOBEC3B. SiHBV was used as controls. Four days post-transfection, cells were treated two times with Pam3CSK4 (100ng/mL) for a total exposure time of 6 days. **A)** extinction of APOBEC3B RNAs was assessed by RT-qPCR, expressed in percentage, normalized to housekeeping gene level and non-treated si-control condition (NT siCtrl). **B)** HBV RNAs were quantified by RT-qPCR, expressed in percentage, normalized to housekeeping gene level and non-treated si control condition (NT siCtrl); effects on HBV antigens were quantified by ELISA in supernatants, expressed in percentage and normalized to NT siCtrl; effects on viremia were quantified by qPCR, according to a standard curve (build with dilutions of a plasmid containing the HBV sequence; effect on cccDNA levels was quantified by FRET-qPCR method, expressed in percentage, normalized to NT siCtrl. All histograms represent the mean of two independent experiments with three biological replicates and the error bars indicate SD.

Figure Sup 13

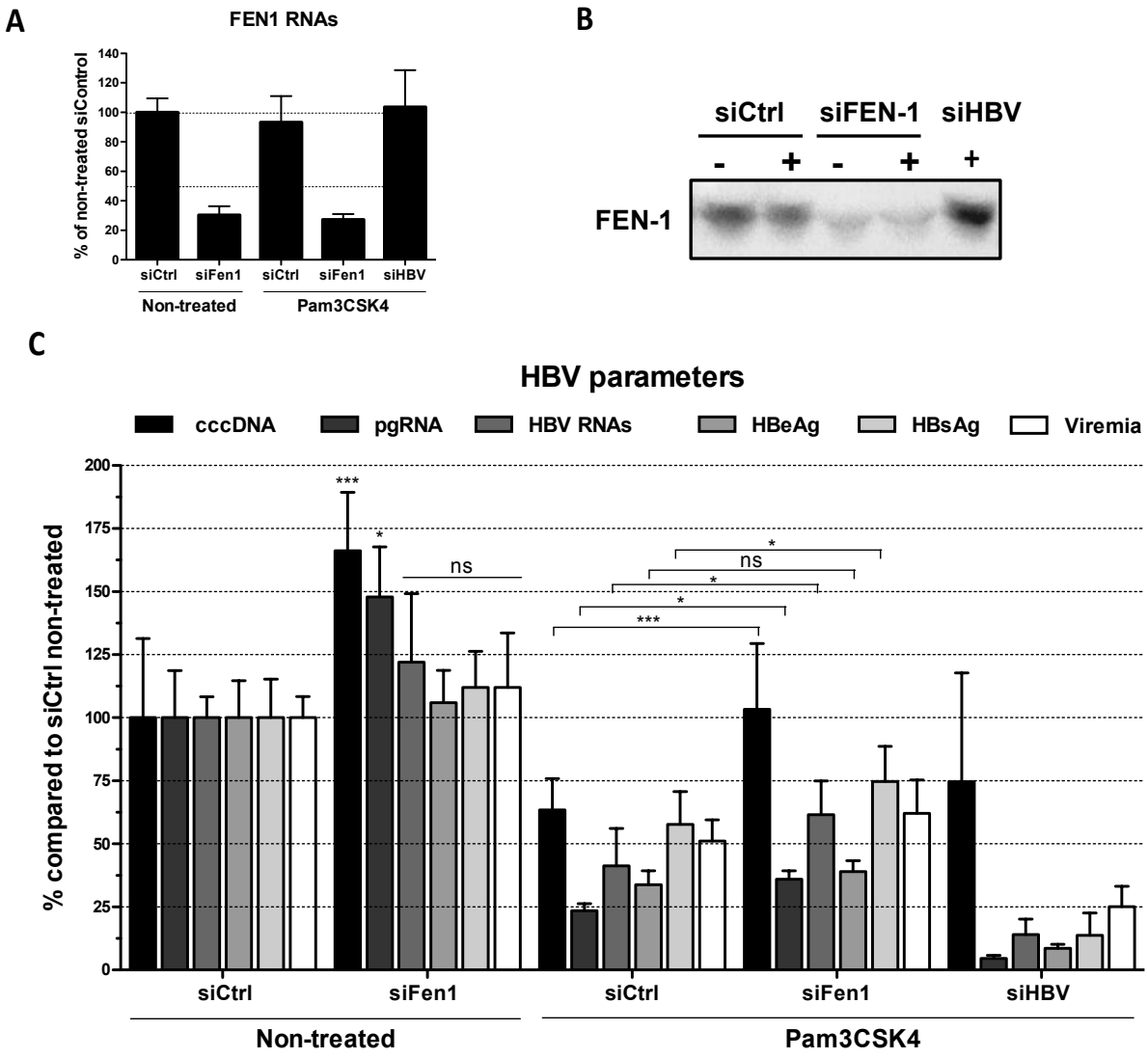

Figure Sup 13. FEN-1 is a host-factor involved in Pam3CSK4-induced phenotype on cccDNA accumulation. Differentiated HepaRG were infected and at least 7 days post infection, cells were transfected once with siRNAs directed to FEN-1. SiHBV was used as controls. Four days post-transfection, cells were either treated two times with Pam3CSK4 (100ng/mL) or left non treated for a total exposure time of 6 days. Effect of siRNA transfection on FEN-1 expression was checked by RT-qPCR (A) and western blotting (B). The effect on cccDNA, HBV pgRNA, HBV total RNAs, secreted HBV antigens, and viremia were respectively quantified by cccDNA-specific-qPCR, RT-qPCR, CLIA, and qPCR. All histograms represent the mean of three independent experiments with three biological replicates and the error bars indicate SD. Statistically significant differences from NT siCtrl (for siFEN-1 NT) or siCtrl (for siFEN-1) conditions are indicated by asterisks (ns: non-significant, *P<0.05, **P<0.005, ***P<0.001).

Figure Sup 14

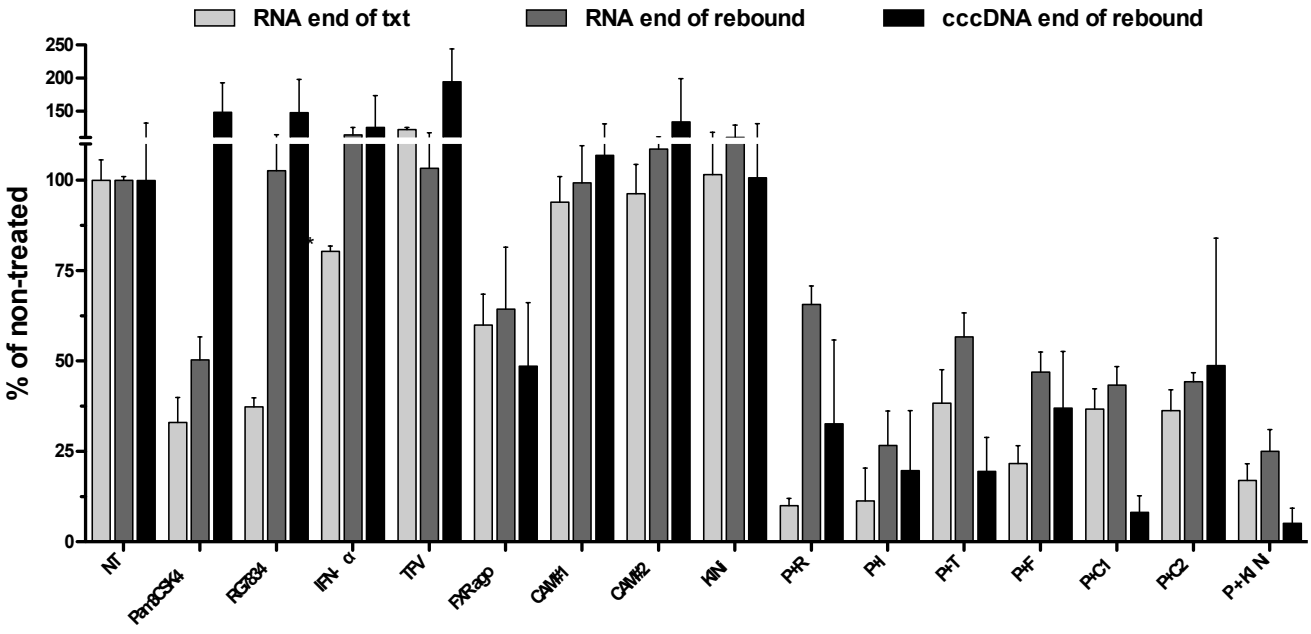

Figure Sup 14. Long lasting effect of combinations of Pam3CSK4 with approved, clinically trialed and investigational drugs. Seven days post-infection, dHepaRG cells were treated twice either with drugs (Pam3CSK4 (P; 25ng/mL), RG7834 (100nM) IFN-α (I; 50IU/ml), TFV (T; 1 µM), FXR-α agonist (F; 100 nM), JNJ-827 (C1, 1µM), JNJ-890 (C2; 1µM), and a kinase inhibitor, (KINi; 5 µM)) in mono-, bi-therapies with the same concentrations, for a total exposure of treatment of 6 days. Indicated HBV parameters were analyzed 14 days post-infection (at the end of treatment), and 24 days post-infection. All histograms represent the mean of one experiment with three biological replicates and the error bars indicate SD.